T-1031

A MOBILITY RATIO STUDY

FOR IMMISCIBLE WATER-OIL SYSTEMS

by

Harold P. Meabon

ProQuest LLC.
789 East Eisenhower Parkway
P.O. Box 1346
Ann Arbor, MI 48106 – 1346

T-1031

A Thesis submitted to the Faculty and the Board of Trustees of the Colorado School of Mines in partial fulfillment of the requirements for the degree of Master of Science in Petroleum Engineering.

Signed: Harold P Meabon
Harold P. Meabon

Golden, Colorado
April 19, 1965

Approved: W. C. Sheldon
W. C. Sheldon
Thesis Advisor

D. M. Bass
D. M. Bass
Head, Department of
Petroleum Engineering

Golden, Colorado
April 19, 1965

ABSTRACT

Areal sweep efficiency at displacing phase breakthrough for a fixed well arrangement is normally correlated with a mobility ratio. These two factors have been correlated in the past by using various models. Only a few investigations have been reported in which flow characteristics were analogus to immiscible systems. In these limited number of cases, mobility ratio variation usually resulted from a change in viscosity ratio rather than a change in rock properties.

Ten distinct rock systems portraying wide variations in water-oil relative permeability characteristics were used in a five-spot mathematical model, simulating channel flow theory. A particular rock system was made to simulate different mobility character by changing the displaced phase viscosity. The results of the model study are discussed in terms of four different mobility ratios. Each mobility ratio has been either mentioned or suggested by others in the literature.

A single mobility ratio was defined which uniquely described the relative conductivity changes within the ten different rock systems. The simply defined mobility ratio will describe two-phase flow in

five-spot systems. It is the ratio of displaced phase relative mobility ahead of the front divided by the displacing phase relative mobility, the latter at average displacing phase saturation behind the front. This definition for immiscible systems has been stated previously in the literature.

CONTENTS

LIST OF TABLES AND FIGURES

ACKNOWLEDGEMENTS

The author expresses his sincere gratitude to Mr. W. C. Sheldon, the Technical Thesis Advisor, and Professor D. M. Bass, the Administrative Advisor. These two gentlemen gave freely of their time and guidance.

Thanks are extended to Professor R. V. Hughes (Ex-officio, Graduate Council Representative) and Professor J. H. Gore for their critical examination of this study.

The author is indebted to the Marathon Oil Company Denver Research Center for the use of their computer, and the various operating divisions for supplying the basic data.

Grateful acknowledgement is made to Mr. L. D. Traupe and those at Marathon who helped prepare the final draft; especially Mrs. Virginia L. Jobes, Messrs. S. G. Detrick, M. K. Taylor, E. C. Rear, R. D. Holly, and R. C. Knight.

INTRODUCTION

Fluids are injected into oil reservoirs to displace oil toward producing wells. Quite often the injected fluid is water or gas and is called the displacing phase. The displacing phase will "push" or displace the oil. Unfortunately, the process is not piston-like for most field systems, and oil in varying amounts is left behind with the injected phase. In this type of displacement a frontal interface normally builds between the displacing phase and the displaced phase. Between this front and the injection well is a saturation gradient. This is a simple description of an immiscible displacement mechanism.

The magnitude and distribution of the saturation gradient depends upon the fluid viscosities and the relative permeability effects for the fluids in the rock system. The complex conductivity distribution is a controlling factor for the area swept by the displacing phase at the time it arrives at a producing well. Other controlling factors include the injection and producing well arrangement, and the relative injection and producing rates for all wells in the system.

It is important to a petroleum engineer to know what fraction of an oil field will be swept by the injected fluid. The economic success of an injection program is related to the volume contacted by the injected fluid.

Repeated five-spot systems have been used as flow models by experimental workers. In so doing they have presented area swept at displacing phase breakthrough as a function of some mobility ratio. The models used in the past, as well as the model used in this study, have assumed complete vertical sweep efficiency. Therefore, the volume swept is proportional to the area swept.

In the strictest sense, two phase mobility ratio is defined as the relative mobility ratio of the two fluids at a single saturation plane within a flow system. This definition is illustrated in the denominator of the simplified fractional flow equation:

$$f_d = \frac{1}{1 + \frac{k_{ro}}{k_{rd}} \cdot \frac{\mu_d}{\mu_o}}$$

where:

subscript d represents the displacing phase.

In presenting results of displacement models, investigators have defined an over-all system mobility ratio. For miscible fluid displacement, the relative permeability of the displaced and displacing phases are regarded as equal. In this case mobility ratio has been defined

as the viscosity ratio of the displacing and displaced phase.

Immiscible displacement doesn't offer such simplicity because saturation gradients exist within the displacing phase region. So, investigators have defined several different system mobility ratios for a two phase displacement. These normally are expressed as a displaced phase relative mobility ahead of the front divided by some relative mobility representing the displacing phase behind the front. In all cases the displaced phase relative mobility is defined as the ratio of relative permeability to viscosity ahead of the front. The displacing phase relative mobility has been defined within the region of the displacing phase, but, at different saturation planes. It has been defined at saturation planes represented by the displacing phase front, average displacing phase saturation behind the front, and at the residual saturation of the displaced phase. Also, it has been defined by using the integrated average conductivity of the fluids behind the front. It may include as a partial sum, the relative mobility of the displaced phase within the region behind the front.

It is obvious that mobility ratio, per se, can have many values. This study concludes that a single value of mobility ratio can be defined that will describe areal sweep efficiency.

Previous Studies

Areal sweep efficiency has been correlated with mobility ratio

by several experimental workers. Areal sweep efficiency is defined as total area swept divided by the total area of the pattern. Mobility ratio is easily defined but, the particular one to use is difficult to ascertain. The purpose of this study was to define a single value of mobility ratio that would properly express relative conductivity changes within a system.

Aronofsky (1952) studied mobility ratio and its influence on flood patterns using a potentiometric model. This model simulated an abrupt front between the displacing and displaced phase. At a later date, Aronofsky (1956) conducted experiments, using the potentiometric model, in which he developed a curve of areal sweep at breakthrough expressed as a function of mobility ratio for a repeated five-spot pattern. He defined mobility ratio as relative mobility of displacing phase divided by relative mobility of the displaced phase. Changes in mobility ratio were simulated by a step-wise procedure of changing the depth of the electrolyte behind the mapped front position. Nobles and Janzen (1958) used a resistance network for studying the mobility ratio effects on areal sweep. Their results parallel the work of Aronofsky.

Cheek and Menzie (1955) used the fluid mapper, Heli-Shaw model, to make similar studies. Their results were different than the previous investigators. Here, the fluids used were miscible and a sharp fluid change existed between the displaced and the displacing phase. The viscosity ratios of the displacing and displaced phases were changed to vary mobility ratios.

Slobod and Caudle (1952) used the X-ray shadowgraph, a new and revolutionary technique, to conduct areal sweepout experiments for a five-spot pattern. A fused Alundum plate was used for the porous media. Most of their work was conducted with miscible systems. They did, however, present four data points for immiscible systems. The X-ray technique allowed them to take continuous pictures of the displacement sequence. At the moment of displacing phase breakthrough they were able to planimeter the swept area and calculate sweepout efficiencies. Caudle, Erickson and Slobod (1955) used the X-ray shadowgraph technique to make sweepout studies of injected fluids beyond the normal well pattern. Here, again, a miscible fluid system was used in an Alundum plate model.

Dyes and Braun (1954) used the X-ray shadowgraph technique with porous plates as their porous media. In this study water, oil and gas comprised the fluid system. The purpose of the investigation was to show the effects of water flooding in the presence of an initial gas phase such as one would find by initiating a water flood in a depleted oil reservoir. They found 100 percent sweepout by the oil bank front at oil bank breakthrough. The areal sweep efficiency at water breakthrough was only slightly improved with a gas phase present. They point out that sweepout pattern data available on virgin reservoirs (two-phase) will suffice as a guide in predicting the behavior of floods in depleted reservoirs.

Dyes, Caudle and Erickson (1954) used the X-ray shadowgraph technique, and Alundum plates with miscible fluids for five-spot systems. The study went beyond the breakthrough conditions and investigated the increased areal sweep efficiency with continued injection. Their experiments indicate that 100 percent areal sweep can ultimately be obtained for some oil field systems.

Craig, Geffen and Morse (1955) used the X-ray shadowgraph technique with a five-spot system to study areal sweep at breakthrough as a function of mobility ratio. They defined mobility ratio as relative mobility of displaced phase ahead of the front divided by relative mobility of the displacing phase behind the front at average displacing phase saturation. A system of consolidated sandstone and immiscible fluids were used to model the experiment. Several definitions of system mobility ratio were tried in correlating their work of immiscible systems with the previous work of Dyes, Caudle and Erickson (1954). An excellent correlation was obtained between immiscible and miscible systems when the displacing phase relative mobility was defined at the average displacing phase saturation behind the front. They extended their experiments beyond the breakthrough phase and studied the increase in areal sweep efficiency with continued injection. The extended work indicated very high areal sweep efficiencies at the economic limit.

These later studies have revealed that areal sweep efficiency

at displacing phase breakthrough for most field conditions is of academic importance, representing a minimum value. This point is well demonstrated by the work of Cotman, Steele and Crawford (1962) in which they compare five-spot and nine-spot performance. The difference in the point of breakthrough and the point of water-oil ratio equal to five represents a relatively small injection volume increment after breakthrough. Several investigators have noted that once breakthrough is reached, it is a very short time, experimentally, until the whole five-spot pattern is swept.

Higgins and Leighton (1961) presented a new concept of modeling. Their work is not concerned with areal sweep efficiency per se. The technique models over-all performance of five-spot (or other) systems under an injection program. In a recent series of papers Higgins and Leighton (1962) and Higgins and Leighton (1963, U. S. Bureau of Mines, RI-6305) have defined their model and techniques of making predictions. They have been able to correlate performance with both laboratory and analytical predictions by Douglas, Peaceman and Rachford (1959).

Purpose and Scope

The objective of this study was to test if a mobility ratio could be defined that would uniquely describe the relative conductivity changes within an immiscible system. Most of the foregoing investigators used either miscible or immiscible fluids with a single rock system. It did not appear that all of their definitions of mobility ratio would

necessarily describe other systems. If a single mobility ratio can be defined that will uniquely define the relative conductivity distribution within any given immiscible system, then variations of relative permeability relationships should not affect correlation of areal sweep efficiency at breakthrough with that mobility ratio.

Craig, Geffen and Morse (1955) did use an immiscible system with consolidated sand. They were able to correlate their work with Dyes, Caudle and Erickson (1954). Their definition of mobility ratio is one of four defined in this study.

The mathematical model used for this study was an octant of a repeated five-spot pattern. It is described by Higgins and Leighton (1962) and will be referred to, hereafter, as H-L model. Ten different rock systems described by individual water-oil relative permeability curves represented the porous media.

This study was a mobility ratio study. Its purpose was to investigate the many definitions of mobility ratio and find one that would describe the total system. Therefore, areal sweep results from the study are not correlated with data presented by other experimental workers.

IMMISCIBLE DISPLACEMENT MECHANISMS

Several of todays petroleum engineering textbooks discuss the theory of miscible and immiscible mechanisms. It is beyond the scope of this paper to review the theory. It is important, however, that one understands the concept of changing conductivities within the swept portion of an immiscible system.

Consider a linear system in which water is displacing oil. The initial condition is oil flowing in the presence of a uniform immobile water saturation. The conductivity of the oil is defined by the effective oil permeability value or its relative permeability value times the rock's specific permeability. The mobility of the oil at initial conditions is k_o / μ_o or its relative mobility, k_{ro} / μ_o. Oil mobility is constant along the flow length of the system since a uniform saturation distribution is assumed.

Water, the displacing phase, is injected at one end of the system and its entry is distributed evenly across the injection face. For the purpose of illustration, capillary and gravity effects are neglected. A distinct front builds between the displacing and displaced phases.

Ahead of the front the oil saturation remains constant as defined initially. Behind the front, along the flow path back to the injection face, there is a saturation gradient. The gradient is one of increasing water saturation and decreasing oil saturation (relative to the front position). A displacing or displaced phase conductivity for every saturation plane along the flow path can be specified. Likewise, a relative mobility can be specified.

The curve M_T in Figure 1, page 11, describes pictorially, total relative mobility of the displacing and displaced phases behind the flood front. The abscissa is the relative distance (X_R) from the injection face to the flood front. Total relative mobility at a point is the sum of the displacing and displaced phase relative mobility at the saturation existing at the point.

$$(M_T)_{X_R} = \left(\frac{k_{ro}}{\mu_o} + \frac{k_{rw}}{\mu_w} \right)_{(S_w)_{X_R}}$$

Viscosity is truly a function of pressure, but, is assumed a constant value along the flow path.

The mobility ratio M' can be defined as the ratio of the displaced phase relative mobility (k_{ro} / μ_o) ahead of the front to the total mobility at a point within the swept region.

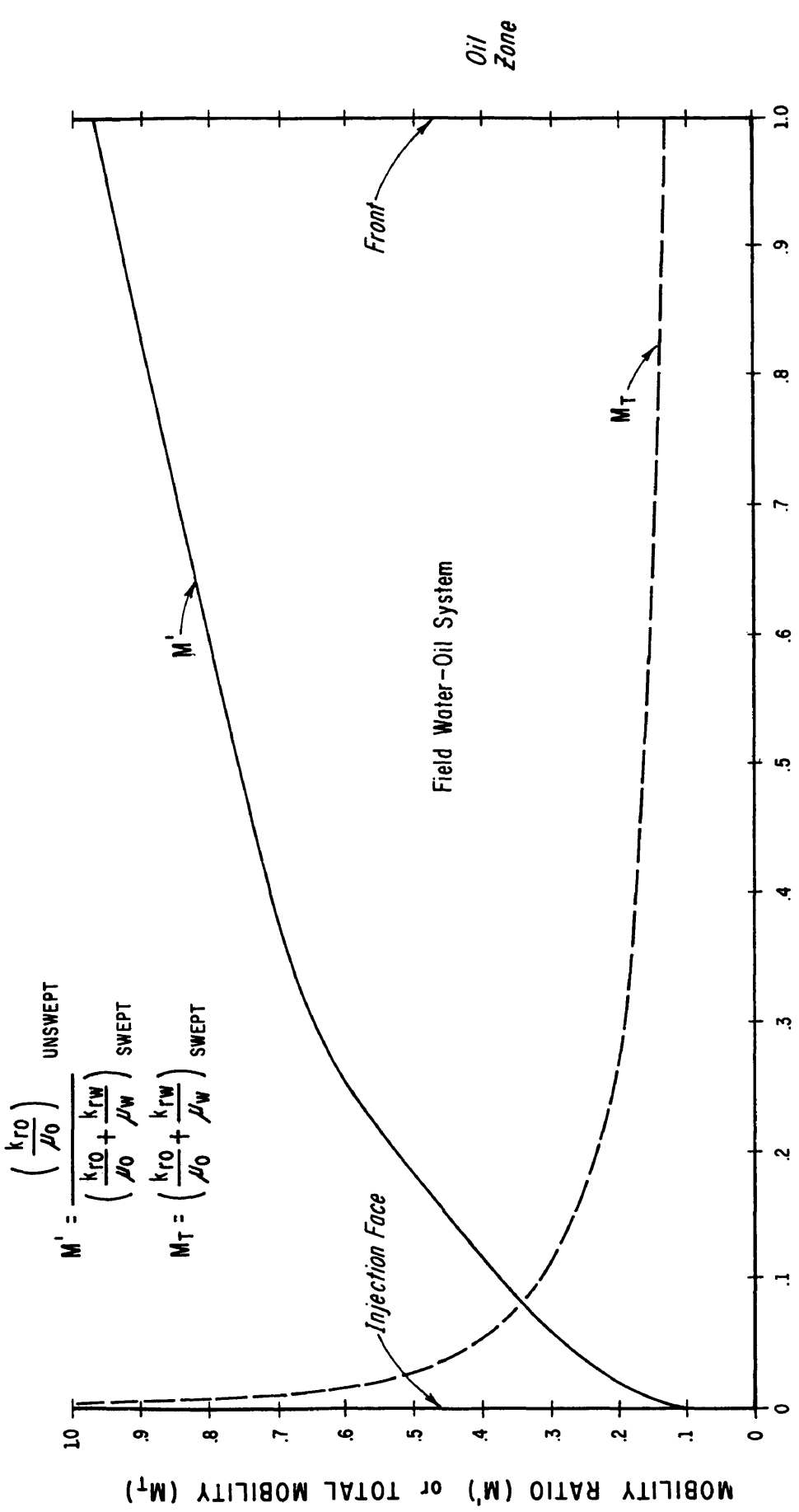

FIGURE 1. MOBILITY RATIO AND TOTAL MOBILITY BEHIND THE FRONT AT A RELATIVE DISTANCE FROM THE INJECTION FACE TO THE FRONT.

$$(M')_{X_R} = \frac{\left(\frac{k_{ro}}{\mu_o}\right)_{\text{ahead of front}}}{(M_T)_{X_R}}$$

The above value truly defines a mobility ratio relative to a point behind the front for the assumed system. In describing mobility ratio, either effective or relative permeability values can be used since specific permeability would cancel from both the numerator and denominator.

By contrast, curves M' and M_T would be horizontal lines in the swept region for miscible systems.

The standard AIME letter symbols, 1956, states the following:

> When the mobilities involved are on opposite sides of an interface, the mobility ratio will be defined as the ratio of the displacing phase mobility to the displaced mobility, or the ratio of the upstream mobility to the downstream mobility (M).

Many mobility studies prior to 1956 referred to the reciprocal of the AIME definition. Therefore, the four mobility ratios defined in this paper are reciprocal values and defined as M'.

$$M' = \frac{1}{M}$$

Mobility Ratio for Immiscible Systems

The curves in Figure 1 present the difficulties in selecting a single mobility ratio; especially when it must represent the system.

Four definitions of mobility ratio were used for correlating purposes. They have either been defined or discussed in the literature. In all cases, the relative mobility ahead of the front is defined as

$$\left(\frac{k_{ro}}{\mu_o}\right)_a.$$

Mobility Ratio 1 (M_1')

When favorable displacement conditions exist, the displaced phase saturation behind the front is low. The displaced phase is said to be relatively immobile behind the front becoming immobile at residual saturation. For this case mobility of the displacing phase alone might describe the mobility behind the front. The integrated average expression for relative permeability to water is used.

$$M_1' = \frac{\left(\frac{k_{ro}}{\mu_o}\right)_a}{\left(\frac{\bar{k}_{rw}}{\mu_w}\right)_b}$$

where:

$\bar{k}_{rw}$ = Integrated average relative permeability to water in the invaded zone, method presented by Higgins and Leighton (1962).

(a) = Ahead of the front

(b) = Behind the front

Mobility Ratio 2 (M_2')

M_2' is defined similar to M_1', but includes the integrated average relative permeability to oil behind the front. When the displacement efficiency is low, relatively high displaced phase saturations exist behind the front. For this reason the displaced phase relative mobility should be included for defining the mobility behind the front. Mobility ratio M_2' is a more rigorous definition of the four presented.

$$M_2' = \frac{\left(\frac{k_{ro}}{\mu_o}\right)_a}{\left(\frac{\bar{k}_{rw}}{\mu_w} + \frac{\bar{k}_{ro}}{\mu_o}\right)_b}$$

where:

$\bar{k}_{ro}$ = Integrated average relative permeability to oil in the invaded zone, method presented by Higgins and Leighton (1962).

Mobility Ratio 3 (M_3')

This mobility ratio has been suggested by Slobod and Caudle (1952) and Craig, Geffen and Morse (1955). The average mobility behind the front is a function of the relative water conductivity at the average water saturation behind the front at breakthrough.

$$M_3' = \frac{\left(\frac{k_{ro}}{\mu_o}\right)_a}{\left(\frac{k'_{rw}}{\mu_w}\right)_b}$$

where:

k'_{rw} = Relative permeability to water at the average water saturation behind the front. The value can be obtained by tangent construct to the fractional flow curve.

Breakthrough is defined at first water production at the production face.

Mobility Ratio 4 (M'_4)

This ratio as defined considers displacing and displaced phase mobility behind the front. The oil mobility is defined at the average water saturation behind the front which is consistent with M'_3. It is presented here as another method of accounting for total mobility behind the front.

$$M'_4 = \frac{\left(\frac{k_{ro}}{\mu_o}\right)_a}{\left(\frac{k'_{rw}}{\mu_w} + \frac{k'_{ro}}{\mu_o}\right)_b}$$

where:

k'_{ro} = Relative permeability to oil at the average water saturation behind the front at breakthrough conditions.

EXPERIMENTAL MODEL

A mathematical model simulating two-phase flow was used to obtain experimental data. It was an octant of a repeated five-spot. The model is described in every detail by Higgins and Leighton (1962). The only modification made was in the use of six channels instead of their described four. Four and six channel model performance has been run by Mr. R. K. Harley and the author, members of the Marathon Oil Company's Production Technology Department. They observed within plotting tolerance, identical results when performance was plotted as pore volumes produced as a function of pore volumes injected. The six channel model replaces channel 1 of the 4 channel H-L model with three smaller channels. The last three channels are similar in each model. It was designed to give more resolution at breakthrough. The six channel geometrical resistivity factors are presented by channel and cell in Table 1, page 36 and 37 of the Appendix.

An octant of a repeated five-spot pattern is shown in the exploded view in 2-C of Figure 2, page 17. Four channels are illustrated instead of the six used in the experiment. The concept of channel flow and the subdivision of the channel into equal volume cells is shown in

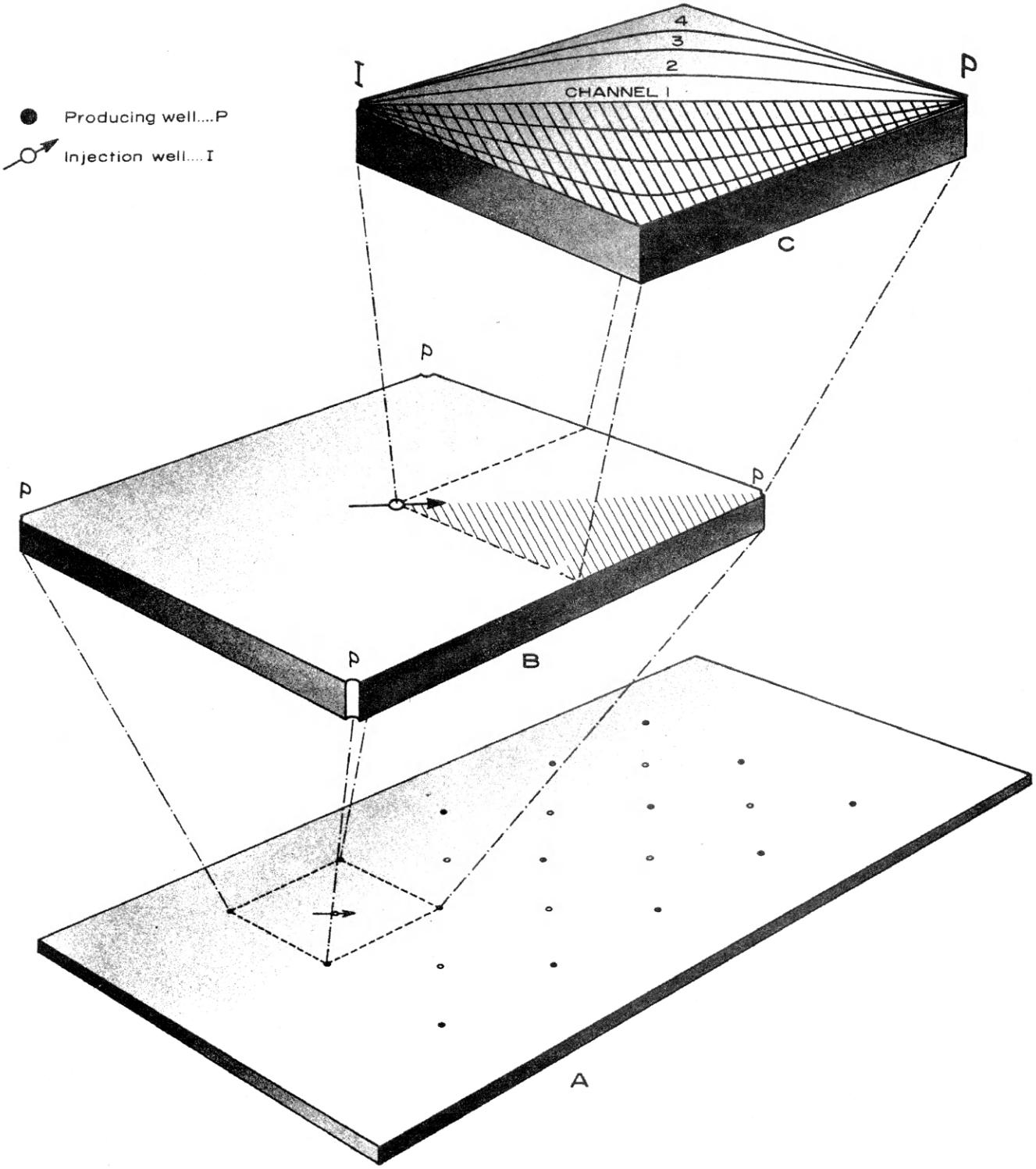

FIGURE 2 SUBDIVISION OF A FIELD 5-SPOT PATTERN INTO FLOW CHANNELS.

Figure 3-A of Figure 3, page 19. The Nth cell shown in 3-B has a linear flow equivalent in 3-C. The individual geometric resistivity factors account for equivalent flow. They have been defined as the mean flow length of the Nth cell divided by its average cross sectional area ($L / \overline{A}$).

Assumptions

The H-L model has a minimum of assumptions as applied to this experiment. The basic assumptions are:

1. Streamlines for a given well configuration are independent of mobility ratio. Therefore, the streamlines determined by a potentiometric model for a mobility ratio of one will set the flow boundaries for the individual channels.
2. No cross flow exists between channels, i.e., streamline flow throughout.
3. Viscosities of flowing phases remain constant throughout the system.
4. No fingers exist within the system.
5. The system has uniform thickness and the rock properties are constant throughout.
6. No gravity or capillary effects.
7. Complete vertical sweep.

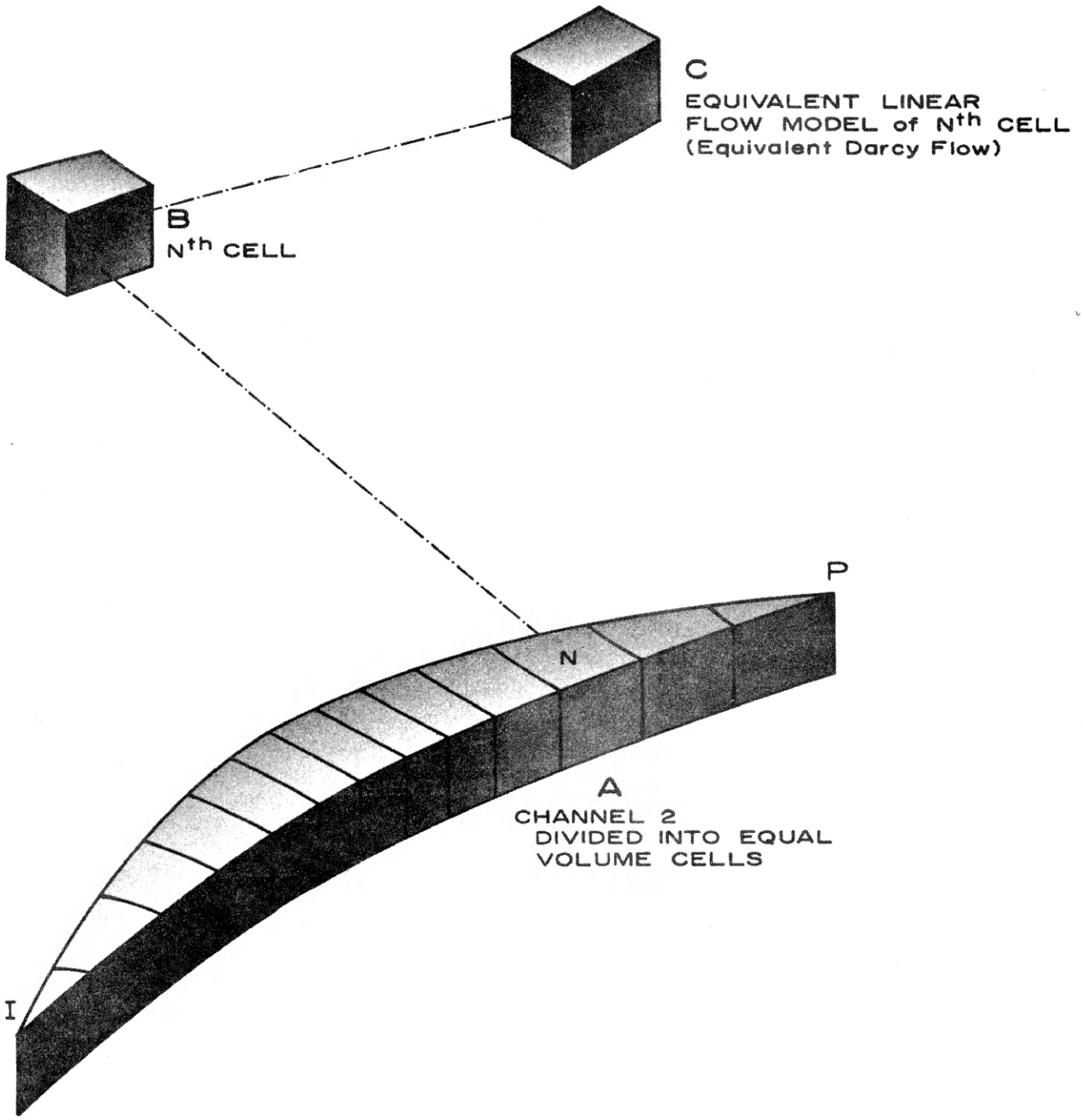

FIGURE 3 SUBDIVISION OF A CHANNEL INTO CELLS AND TRANSFORMATION OF THE ELEMENTAL CELL INTO AN EQUIVALENT LINEAR FLOW MODEL.

Different Systems

Various rock systems were simulated by using different water-oil relative permeability curves. These data help to define the changes in saturations between the injection and producing well.

Ten distinct rock systems were used. The water-oil relative permeability characteristics for these systems are shown in Figure 4, page 21. Nine of the ten sets of relative permeability curves were run in commercial laboratories. Individual phase relative permeability characteristics are tabulated in Tables 2 through 11, pages 38 through 47 of the Appendix. The tables include the individual rock properties for the same specimen used in obtaining relative permeability data. These data comprise actual rock systems and represent oil fields in the United States and Canada. Nine of the ten curves have been identified as to formation and geographical location.

Model Dimensions

The model represents one uniform layer for an octant of a repeated five-spot pattern. The five-spot has an included area of 160 acres. The distance between the injection and producing well is 1867 feet with well bore radius of 0.5 feet. The formation is 25 feet thick.

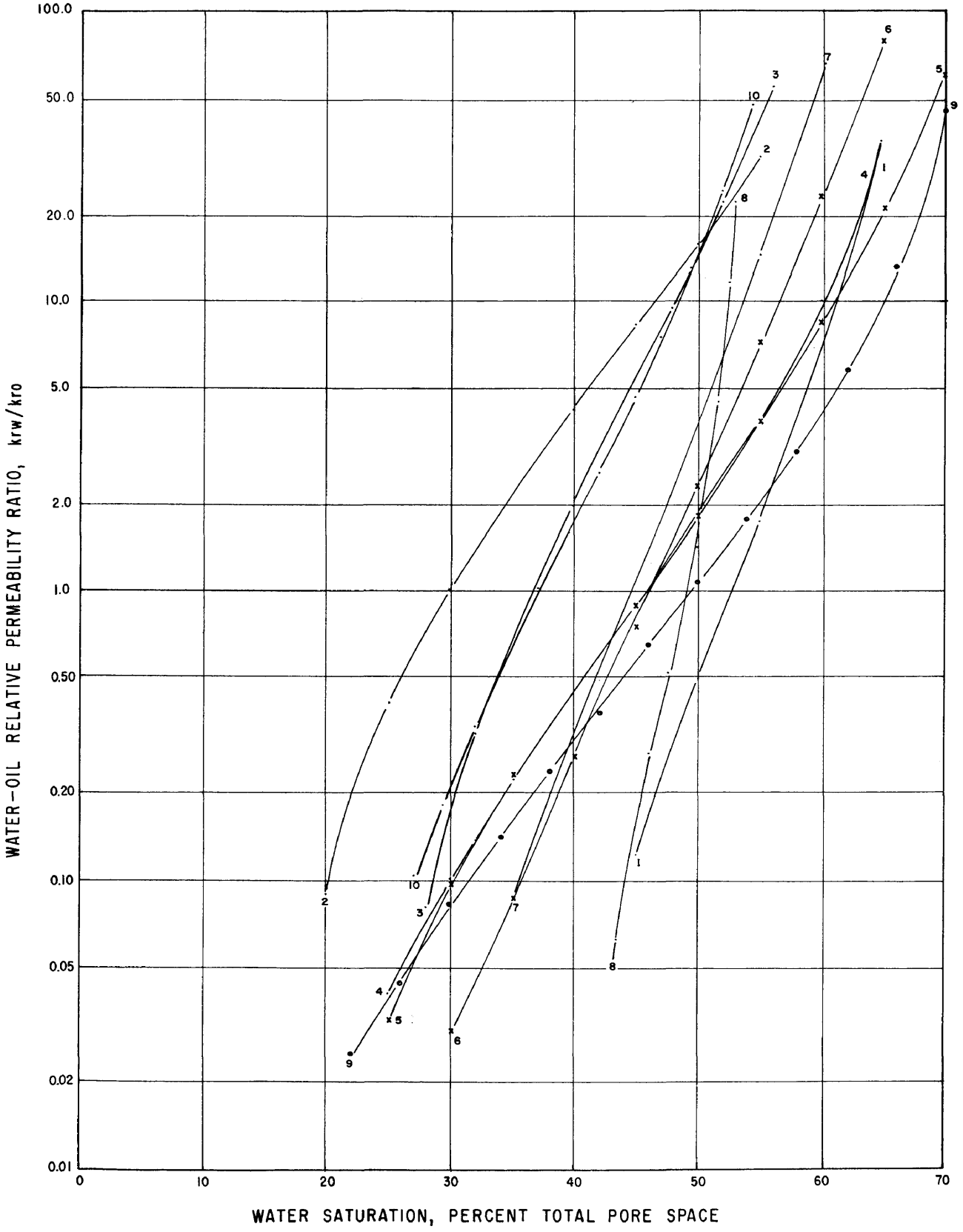

FIGURE 4. WATER-OIL RELATIVE PERMEABILITY CHARACTERISTICS FOR THE TEN DIFFERENT SYSTEMS MODELED.

EXPERIMENTAL PROCEDURE

Digital Computer Program

The H-L model was programmed for a digital computer. The author and an associate wrote the program for Marathon Oil Company. It was programmed for a Burroughs 205 in machine language.

System Variations

Input requirements were basically the rock system. The data were plotted as water and oil relative permeability as a function of water saturation. Input for the computer was read from the smoothed curves for each one percent change in water saturation. A linear table look-up routine retrieved relative permeability information.

Specific permeability, initial immobile water saturation and porosity compatible with the water-oil relative permeability curve were used.

A particular rock system was represented by a water-oil relative permeability curve, specific permeability, initial immobile water saturation and porosity. Mobility ratio for a rock system was varied by changing the oil viscosity. Water viscosity of 0.46 cps was constant for all runs.

Five complete performance curves representing different mobility ratios were run for each rock system. As many as twelve trial oil viscosities were run in order to obtain five acceptable mobility ratios between 0.1 and 10.

The total project represents 50 complete five-spot predictions; ten rock systems, five mobility ratios each.

RESULTS FOR ONE FIVE-SPOT

The following was available from computer output:

1. N_{pbr} = Cumulative oil production at water breakthrough, stock tank barrels.
2. V_p = Pore volume, reservoir barrels.
3. $\bar{S}'_{wbr}$ = Average water saturation at breakthrough by tangent construction with fractional flow (f_w) curve, fractional pore volume.

Areal sweep efficiency, E_{br}, at first water breakthrough was calculated as follows:

$$E_{br} = \frac{\frac{N_{pbr}}{V_p}}{(\bar{S}'_{wbr} - S_{wi})} \times 100, \text{ \% of total 5-spot area swept.}$$

The oil formation volume factor was assumed 1.0. The output included the specific information required to calculate the four previously defined mobility ratios.

All necessary output and calculated information is tabulated in

Tables 12 through 21, pages 49 through 58 of the Appendix. These data contain all information required for plotting figures 5, 6, and 8 through 12, pages 60, 61, and 63 through 67 of the Appendix.

DISCUSSION

From a theoretical point of view, mobility ratio M_2' is rigorously defined. The denominator includes two phases flowing in the swept region. Furthermore, the relative conductivity of each flowing phase is an integrated average. The averaging technique is detailed by Higgins and Leighton (1962). It assumes that the reciprocal of relative permeability represents a resistivity function; fluid flow is analagous to electric flow, therefore, individual resistivities can be added in series; the pressure drop from injection face to front position is the same in the oil and water phase; and finally, the integrated average oil and water relative permeability when properly expressed in separate Darcy flow equations will yield the correct oil and water flow rates flowing from the injection face to the front.

It was not the purpose nor scope of this study to compare the calculated areal sweeps, from the H-L model, with those of other experimental workers. It was the purpose of this study to test if a mobility ratio could be defined that would describe the conductivity distribution within the water-oil system modeled. Mobility ratio M_2'

was defined to represent the total system. The thesis was: if the conductivity distribution is uniquely defined by M_2', identical areal sweeps at breakthrough for equal M_2' values would be reproducible within experimental limits. Figure 5, page 60, is the correlation between breakthrough areal sweep efficiency and M_2'. The least square fit through 50 data points indicated areal sweep efficiencies of 68.65 and 74.70 percent corresponding to M_2' values of 0.1 to 10.0. The standard error of estimate was 0.47 percent.

The 6.05 percent spread is due to the pressure surface being different for various mobility ratios. The individual channels reflect this difference even though the flow boundaries were defined using a mobility ratio of one. Data in Figure 5 proves that mobility ratio M_2' uniquely defines the conductivity distribution for the ten systems studied. It can be stated with reasonable assurance that M_2' will define other immiscible systems with characteristics similar to the ten tested in this study.

Mobility ratio M_3' was previously suggested by Slobod and Caudle (1952) and Craig, Geffen and Morse (1955). It is easy to calculate. One needs only to calculate a few points for a fractional flow curve and obtain the average displacing phase saturation behind the front at or prior to breakthrough. This saturation defines the displacing phase relative permeability. The variation between M_2' and M_3' appears to be small, especially within the range of mobility ratios for actual field systems. Figure 6, page 61, reflects the small differences.

Further comparison of M_2' and M_3' can be made. A correlation of

areal sweep efficiency at breakthrough correlated with M_3' was presented by Craig, Geffen and Morse (1955). It is shown in Figure 7, page 62. The curve was plotted from a figure in the cited reference and does not represent actual data points. Mobility ratio M_2' is defined more rigorously than M_3'. Therefore, sweeps in Figure 7 could be replotted as a function of M_2' by using the correlation in Figure 6. For example, a value of M_3' equal to 1.0 corresponds to a value of M_2' equal to 1.05. The areal sweep value for M_3' of 1.0 is 69.5 percent. This value would have been better represented had it been plotted at M_2' value of 1.05. The sweep value for M_3' of 1.05 is approximately 70 percent. The actual error then is + 0.72 percent. That is, using mobility ratio M_3' instead of M_2' yields slightly more favorable sweep efficiency near M' values of 1.0. The error becomes less for mobility values greater than 1.0 because the correlation in Figure 6 is improved for mobility values greater than 1.0. The error is approximately + 1.5 percent at M_3' values near 0.5. This is well within engineering accuracies.

Mobility ratio M_3' is easy to calculate and correlates well with the definition M_2'. It has been used by earlier investigators. Therefore, it is recommended that M_3' be used to describe the over-all conductivity distribution for immiscible systems.

The integrated average displacing phase relative conductivity is not truly represented by the average displacing phase saturation behind the front. This is shown in Figure 8, page 63. The difference

becomes significant below M_3' values of 1.0. The integrated value is less than the value at a saturation plane represented by the average saturation. This is perhaps better illustrated in Figure 9, page 64.

It could be stated for:

$$k_{rw}' \leq 0.10,\ k_{rw}' > \bar{k}_{rw}$$

$$k_{rw}' > 0.10,\ k_{rw}' \cong \bar{k}_{rw}$$

Mobility ratio M_3' neglects the effects of displaced phase conductivity behind the front at the average displacing phase saturation. M_4' includes this effect. Its omission in calculating M_3' introduces a very small error and can be neglected. This is shown in Figure 10, page 65. There is a reasonable explanation why the displaced phase conductivity can be neglected behind the front. Relatively high displaced phase saturations usually imply an unfavorable displacing efficiency. This is normally synonymous with high values for the displaced phase viscosity. For example, when oil saturations behind the front are high, k_{ro} and μ_o values are relatively high. When oil saturations are low, k_{ro} and μ_o values are relatively low. The effect is to maintain a relatively stable value for oil relative mobility behind the front.

The omission of the integrated average oil relative mobility behind the front is more serious. The mobility ratio M_2' includes it and M_1' does not. The difference can be seen in Figure 11, page 66. The error increases for M_2' values less than 1.0.

Rules of thumbs are often used in the industry. One such rule is that mobility ratio for an immiscible system is approximated by viscosity ratio of displacing and displaced phase. It was discussed earlier that a mobility ratio for miscible systems can be expressed as μ_d / μ_o. Figure 12, page 67, is a correlation of mobility ratio M_2' with oil-water viscosity ratio (μ_o / μ_d). The "fairway" plot contains 90 percent of all data obtained from the study. It well illustrates the pitfall of the synonmous association of viscosity ratio with mobility ratio for immiscible systems. For example, a viscosity ratio of 1000 might represent an average mobility ratio of 0.15. A viscosity ratio of 1.0 might represent an average mobility ratio of 4.0. The implication of 1000 fold change in viscosity ratio reflects approximately a 27 fold change in mobility ratio.

Dyes and Braun (1954) presented a similar plot for oil viscosity. Their data correlates well with Figure 12 when re-calculated in terms of oil-water viscosity ratio. This plot would give an engineer in the field an estimate of mobility ratio if no other data were available to him.

SUMMARY

Areal sweep efficiency at displacing phase breakthrough has been a convenient correlating parameter. It normally has been correlated with a mobility ratio. Areal sweep efficiency at breakthrough is of academic value and represents a minimum value.

Mobility ratio can easily be defined for miscible systems by a simple viscosity ratio. Immiscible systems are more complex. However, a simple mobility ratio can be defined which will uniquely describe immiscible systems. For most engineering work, mobility ratio M_3' is sufficiently accurate.

Actual field oil-water viscosity ratios were estimated for the ten systems. The mobility ratio (M_2') ranged from 0.6 to 4.0. This range is representative of "virgin" oil-water systems. "Sweepout pattern data available on virgin reservoirs will suffice as a guide in predicting the behavior of depleted reservoirs," Dyes and Braun (1954).

In the absence of laboratory data one could estimate mobility ratios for systems using a correlation of mobility ratio M_2' with oil-water viscosity ratio. From this raw estimate the engineer would be able

to classify an injection program as favorable or unfavorable. This approach should never replace the methodical engineering calculations.

CONCLUSIONS

1. The best definition for mobility ratio (M_2') uses integrated average conductivities of both displacing and displaced phases in the swept region. It uniquely describes immiscible two-phase systems.
2. A simple and previously reported mobility ratio (M_3') is acceptable for engineering work. It is the ratio of displaced phase mobility ahead of the front divided by the displacing phase mobility defined at the average displacing phase saturation.
3. Most water floods will fall within the mobility ratio range encountered in the ten systems of this study. Actual field mobility ratios between 0.6 and 4.0 were represented.
4. Mobility ratio estimates can be made from oil-water viscosity ratios. This is <u>not</u> a substitute for the engineering approach.

RECOMMENDATIONS

The Higgins-Leighton digital computer model for a five-spot should be run using a larger number of channels. The work might indicate that a greater variation in sweep efficiency at breakthrough could be obtained for the same range of mobility ratio used in this report.

APPENDIX

Tables 1 through 21

Figures 5 through 12

Table 1

Geometrical Resistivity Factors*
for 160 Acre - Repeated Five-Spot

Cell**	Channel					
	1	2	3	4	5	6
1	227.144	75.701	54.703	25.731	26.756	62.551
2	13.035	4.339	3.127	1.455	1.469	3.275
3	7.706	2.566	1.849	0.856	0.861	1.879
4	5.511	1.835	1.323	0.610	0.606	1.287
5	4.314	1.435	1.031	0.475	0.466	0.952
6	3.560	1.184	0.851	0.390	0.376	0.733
7	3.048	1.014	0.728	0.331	0.313	0.579
8	2.680	0.891	0.638	0.288	0.266	0.464
9	2.404	0.799	0.571	0.256	0.231	0.377
10	2.189	0.728	0.520	0.232	0.203	0.308
11	2.024	0.672	0.479	0.212	0.181	0.253
12	1.891	0.628	0.447	0.196	0.162	0.211
13	1.784	0.592	0.421	0.183	0.147	0.176
14	1.700	0.564	0.400	0.173	0.135	0.149
15	1.633	0.542	0.384	0.164	0.125	0.128
16	1.579	0.524	0.370	0.158	0.116	0.111
17	1.538	0.510	0.360	0.153	0.110	0.099
18	1.509	0.500	0.353	0.149	0.105	0.091
19	1.489	0.494	0.348	0.146	0.101	0.088
20	1.479	0.490	0.346	0.145	0.099	0.091

(continued)

Table 1 (continued)

Cell**	Channel					
	1	2	3	4	5	6
21	1.478	0.490	0.346	0.145	0.099	0.095
22	1.486	0.493	0.348	0.146	0.100	0.087
23	1.504	0.499	0.352	0.148	0.103	0.089
24	1.532	0.508	0.359	0.151	0.108	0.096
25	1.570	0.520	0.368	0.156	0.114	0.107
26	1.621	0.538	0.380	0.162	0.122	0.123
27	1.686	0.559	0.397	0.170	0.132	0.143
28	1.767	0.587	0.417	0.181	0.144	0.169
29	1.871	0.621	0.442	0.193	0.158	0.202
30	2.000	0.664	0.473	0.208	0.176	0.242
31	2.162	0.719	0.513	0.227	0.198	0.295
32	2.371	0.788	0.563	0.252	0.225	0.362
33	2.642	0.878	0.628	0.284	0.260	0.447
34	3.001	0.999	0.717	0.325	0.305	0.560
35	3.505	1.166	0.838	0.383	0.368	0.712
36	4.249	1.413	1.015	0.467	0.456	0.930
37	5.426	1.806	1.301	0.601	0.596	1.264
38	7.588	2.527	1.822	0.844	0.847	1.861
39	12.887	4.289	3.089	1.436	1.452	3.262
40	225.935	75.364	54.440	25.624	26.658	63.588

* Factors based on one foot thickness.
** Cell 1 at injection well and Cell 40 at producing well.

Bulk Volume Per Cell Cubic Feet	528.95	1595.55	2261.92	5347.51	7014.64	5032.30
Included Angle at Injection Well, Degrees	1.512	4.537	6.291	13.473	13.270	5.917

Note: 1867 Feet Between Injection and Producing Well.
Well Bore Radius of 0.50 Feet

Table 2 - Relative Permeability Curves 1
"Bridgeport Sand, Illinois"

k_{air} = 218 mds

$\emptyset$ = 21.9%

S_{wi} = 35.2%

k_o = 182 mds @ S_{wi}

k_w = 38 mds @ S_{or}

S_{or} = 30.0%

μ_o/μ_w = 12, estimated field conditions

$S_{w,\%}$	k_{rw}*	k_{ro}*
42	0.003	0.175
44	0.012	0.142
46	0.020	0.119
48	0.029	0.099
50	0.039	0.079
52	0.049	0.061
54	0.060	0.045
56	0.072	0.032
58	0.084	0.022
60	0.097	0.014
62	0.116	0.009
64	0.130	0.005
66	0.141	0.003
68	0.160	0.001
69.1	0.169	0.001

* Relative to air permeability

Table 3 - Relative Permeability Curves 2

"J-2-A Sand Saskatchewan, Canada"

k_{brine} = 309 mds

ϕ = 20.2%

S_{wi} = 5%

k_o = 309 mds @ S_{wi}

k_w = 150 mds @ S_{or}

S_{or} = 35.0%

μ_o/μ_w = 18, estimated field conditions

S_w,%	k_{rw}	k_{ro}
15	0.0028	0.420
20	0.024	0.272
25	0.071	0.177
30	0.116	0.116
35	0.160	0.074
40	0.204	0.048
45	0.250	0.030
50	0.300	0.019
55	0.353	0.0112

Table 4 - Relative Permeability Curves 3

"Cardium Sand, Alberta, Canada"

k_{air} = 161 mds

ϕ = 24.6%

S_{wi} = 21.8%

k_o = 78 mds @ S_{wi}

k_w = 75 mds @ S_{or}

S_{or} = 36.6%

μ_o/μ_w = 2.2, estimated field conditions

S_w, %	k_{rw}*	k_{ro}*
28	0.015	0.187
32	0.040	0.125
36	0.065	0.093
40	0.124	0.063
44	0.175	0.039
48	0.237	0.025
52	0.295	0.013
56	0.361	0.007
60	0.424	0.003
64	0.490	0.001

* Relative to air permeability

Table 5 - Relative Permeability Curves 4

"Tensleep Sand, Wyoming"

k_{air} = 165 mds

$\emptyset$ = 14.8%

S_{wi} = 11.4%

k_o = 155 mds @ S_{wi}

k_w = 44 mds @ S_{or}

S_{or} = 25.7%

μ_o/μ_w = 25.5, estimated field conditions

S_w, %	k_{rw}*	k_{ro}*
20	0.008	0.640
25	0.019	0.475
30	0.033	0.335
35	0.052	0.235
40	0.075	0.165
45	0.103	0.113
50	0.132	0.043
55	0.163	0.020
60	0.197	0.006
65	0.231	0.001

* Relative to air permeability

Table 6 - Relative Permeability Curves 5

"Darwin Sand, Wyoming"

k_{air} = 116 mds

$\emptyset$ = 16.3%

S_{wi} = 18.7%

k_o = 60 mds @ S_{wi}

k_w = 23 mds @ S_{or}

S_{or} = 21.2%

μ_o/μ_w = 44.5, estimated field conditions

$S_{w,\%}$	k_{rw}*	k_{ro}*
25	0.007	0.214
30	0.012	0.125
35	0.018	0.078
40	0.024	0.053
45	0.030	0.034
50	0.038	0.021
55	0.046	0.012
60	0.057	0.007
65	0.071	0.003
70	0.091	0.001

* Relative to air permeability

Table 7 - Relative Permeability Curves 6

"Muddy Sand, Wyoming"

k_{air} = 10 mds

ϕ = 18.1%

S_{wi} = 21.8%

k_o = 8.1 mds @ S_{wi}

k_w = 4.9 mds @ S_{or}

S_{or} = 25.1%

μ_o/μ_w = 1.7, estimated field conditions

S_w,%	k_{rw}*	k_{ro}*
30	0.006	0.209
35	0.010	0.106
40	0.017	0.063
45	0.030	0.040
50	0.050	0.022
55	0.081	0.011
60	0.134	0.006
65	0.217	0.003
70	0.338	0.001

* Relative to air permeability

Table 8 - Relative Permeability Curves 7

"Dakota Sand, Wyoming"

k_{air} = 53 mds

$\emptyset$ = 17.8%

S_{wi} = 12.1%

k_o = 41 mds @ S_{wi}

k_w = 9 mds @ S_{or}

S_{or} = 32.1%

μ_o/μ_w = 1.7, estimated field conditions

$S_{w,\%}$	k_{rw}*	k_{ro}*
35	0.007	0.082
40	0.017	0.052
45	0.035	0.031
50	0.063	0.017
55	0.096	0.007
60	0.136	0.002
65	0.182	0.0005

* Relative to air permeability

Table 9 - Relative Permeability Curves 8

"J-Sand, Nebraska"

k_{air} = 147 mds

$\emptyset$ = 17.4%

S_{wi} = 29.7%

k_o = 137 mds @ S_{wi}

k_w = 20 mds @ S_{or}

S_{or} = 43.5%

μ_o/μ_w = 3.7, estimated field conditions

$S_{w,\%}$	k_{rw}*	k_{ro}*
43.6	0.008	0.132
46.2	0.024	0.087
47.6	0.033	0.064
49.9	0.053	0.037
51.4	0.076	0.018
52.5	0.096	0.008
53.0	0.103	0.005
54.1	0.120	0.001

* Relative to air permeability

Table 10 - Relative Permeability Curves 9

"D-Sand, Nebraska"

k_{air} = 963 mds

ϕ = 22.7%

S_{wi} = 7.7%

k_o = 893 mds @ S_{wi}

k_w = 374 mds @ S_{or}

S_{or} = 24.3%

μ_o/μ_w = 3.7, estimated field conditions

$S_{w,\%}$	k_{rw}*	k_{ro}*
22	0.014	0.570
26	0.021	0.489
30	0.034	0.417
34	0.049	0.348
38	0.067	0.286
42	0.087	0.231
46	0.117	0.182
50	0.146	0.139
54	0.179	0.102
58	0.215	0.071
62	0.245	0.043
66	0.283	0.022
70	0.326	0.008

* Relative to air permeability

Table 11 - Relative Permeability Curves 10

"Curve 10"

k_{air} = 2039 mds

ϕ = 33.6%

S_{wi} = 9.0%

k_o = 1929 mds @ S_{wi}

k_w = 830 mds @ S_{or}

S_{or} = 39.9%

μ_o/μ_w = 1.6, estimated field conditions

$S_{w,\%}$	k_{rw}*	k_{ro}*
27	0.023	0.225
29.5	0.032	0.181
32.0	0.049	0.147
34.5	0.070	0.115
37.0	0.091	0.091
39.5	0.113	0.072
42.0	0.140	0.055
44.5	0.177	0.040
47.0	0.209	0.028
49.5	0.240	0.018
52.0	0.278	0.012
54.5	0.312	0.006
57.0	0.350	0.003
58.1	0.366	0.002

* Relative to air permeability

Nomenclature for Tables 12 through 21

μ_o = Oil viscosity, cps.

μ_w = Water viscosity, cps.

$\bar{S}'_{wbr}$ = Average water saturation at breakthrough by tangent construction with fractional flow (f_w) curve, fractional pore volume.

$\bar{S}_{wbr}$ = Integrated average water saturation at breakthrough, fractional pore volume.

k_{ro} = Relative permeability to oil in uninvaded zone at initial water saturation.

$\bar{k}_{ro}$ = Integrated average relative permeability to oil in the invaded zone (method presented by Higgins and Leighton (1962).

k'_{ro} = Relative permeability to oil in the invaded zone at $\bar{S}'_{wbr}$.

$\bar{k}_{rw}$ = Integrated average relative permeability to water in the invaded zone (method presented by Higgins and Leighton (1962).

k'_{rw} = Relative permeability to water in the invaded zone at $\bar{S}'_{wbr}$.

M'_1 = $(k_{ro} / \mu_o) \div (\bar{k}_{rw} / \mu_w)$.

M'_2 = $(k_{ro} / \mu_o) \div (\bar{k}_{rw} / \mu_w + \bar{k}_{ro} / \mu_o)$.

M'_3 = $(k_{ro} / \mu_o) \div (k'_{rw} / \mu_w)$.

M'_4 = $(k_{ro} / \mu_o) \div (k'_{rw} / \mu_w + k'_{ro} / \mu_o)$.

N_{pbr} = Cumulative oil production at water breakthrough, stock tank barrels (for this study N_{pbr} represents oil production from one developed 5-spot pattern).

V_p = Pore volume (one developed 5-spot pattern), reservoir barrels.

S_{wi} = Initial water saturation at start of flood (for this study S_{wi} is considered immobile), fractional pore volume.

E_{br} = Areal sweep efficiency at breakthrough, percent of total pattern affected.

Table 12 - Relative Permeability Curves 1
Displacement Results
"Bridgeport Sand, Illinois"

	Results of Computer Runs				
	1	2	3	4	5
μ_o/μ_w	217.4	25.0	2.17	0.326	0.152
μ_o	100	11.5	1.0	0.150	0.070
μ_w	0.460	0.460	0.460	0.460	0.460
$\bar{S}'_{wbr}$	0.424	0.482	0.603	0.674	0.692
$\bar{S}_{wbr}$	0.423	0.481	0.603	0.673	0.690
k_{ro}	0.295	0.295	0.295	0.295	0.295
$\bar{k}_{ro}$	0.161	0.0684	0.00303	0.000452	0.000230
k'_{ro}	0.166	0.0938	0.0136	0.0131	0.00034
$\bar{k}_{rw}$	0.00436	0.0236	0.0934	0.151	0.167
k'_{rw}	0.00641	0.0301	0.0971	0.153	0.170
M'_1	0.311	0.499	1.45	5.99	11.6
M'_2	0.266	0.447	1.43	5.93	11.5
M'_3	0.212	0.393	1.40	5.92	11.4
M'_4	0.189	0.349	1.31	5.77	11.2
$N_{pbr} \times 10^6$	0.340	0.628	1.23	1.62	1.71
$V_p \times 10^6$	6.796	6.796	6.796	6.796	6.796
N_p/V_p	0.0500	0.0924	0.181	0.238	0.252
S_{wi}	0.352	0.352	0.352	0.352	0.352
$(S'_{wbr} - S_{wi})$	0.0712	0.129	0.251	0.321	0.338
E_{br}	70.2	71.4	72.1	74.1	74.7

Table 13 - Relative Permeability Curves 2
Displacement Results
"J-2-A Sand Saskatchewan, Canada"

	Results of Computer Runs				
	1	2	3	4	5
μ_o/μ_w	326	109	17.8	1.0	0.326
μ_o	150	50.0	8.20	0.460	0.150
μ_w	0.460	0.460	0.460	0.460	0.460
$\bar{S}'_{wbr}$	0.196	0.214	0.269	0.481	0.587
$\bar{S}_{wbr}$	0.195	0.214	0.268	0.480	0.581
k_{ro}	1.00	1.00	1.00	1.00	1.00
$\bar{k}_{ro}$	0.280	0.233	0.129	0.00135	0.000405
k'_{ro}	0.283	0.263	0.151	0.129	0.00717
$\bar{k}_{rw}$	0.0148	0.0299	0.0729	0.265	0.385
k'_{rw}	0.0205	0.0290	0.0887	0.0224	0.402
M'_1	0.207	0.308	0.770	3.78	7.97
M'_2	0.195	0.287	0.700	3.76	7.94
M'_3	0.149	0.318	0.633	3.56	7.64
M'_4	0.144	0.293	0.578	3.30	7.24
$N_{pbr} \times 10^6$	0.633	0.719	0.972	1.98	2.50
$V_p \times 10^6$	6.269	6.269	6.269	6.269	6.269
N_p/V_p	0.101	0.115	0.155	0.315	0.398
S_{wi}	0.05	0.05	0.05	0.05	0.05
$(\bar{S}'_{wbr} - S_{wi})$	0.145	0.164	0.218	0.429	0.531
E_{br}	69.4	69.9	71.1	73.4	75.0

Table 14 - Relative Permeability Curves 3
Displacement Results
"Cardium Sand, Alberta, Canada"

	Results of Computer Runs				
	1	2	3	4	5
μ_o/μ_w	21.7	2.17	1.09	0.217	0.087
μ_o	10.0	1.00	0.500	0.100	0.040
μ_w	0.460	0.460	0.460	0.460	0.460
$\overline{S}'_{wbr}$	0.317	0.440	0.485	0.583	0.629
$\overline{S}_{wbr}$	0.317	0.440	0.484	0.580	0.624
k_{ro}	0.329	0.329	0.329	0.329	0.329
$\overline{k}_{ro}$	0.126	0.0127	0.00623	0.00120	0.000498
k'_{ro}	0.141	0.0407	0.0227	0.00356	0.000912
$\overline{k}_{rw}$	0.0269	0.151	0.218	0.378	0.458
k'_{rw}	0.0374	0.174	0.238	0.387	0.459
M'_1	0.563	1.00	1.39	4.00	8.28
M'_2	0.464	0.965	1.36	3.95	8.18
M'_3	0.405	0.873	1.27	3.90	8.26
M'_4	0.345	0.787	1.17	3.74	8.08
$N_{pbr} \times 10^6$	0.531	1.21	1.46	2.05	2.32
$V_p \times 10^6$	7.63	7.63	7.63	7.63	7.63
N_p/V_p	0.0696	0.158	0.191	0.268	0.304
S_{wi}	0.218	0.218	0.218	0.218	0.218
$(\overline{S}'_{wbr} - S_{wi})$	0.0987	0.222	0.266	0.362	0.406
E_{br}	70.5	71.4	72.0	74.1	74.9

Table 15 - Relative Permeability Curves 4
Displacement Results
"Tensleep Sand, Wyoming"

	Results of Computer Runs				
	1	2	3	4	5
μ_o/μ_w	435	21.7	2.17	1.09	0.430
μ_o	200	10.0	1.00	0.500	0.200
μ_w	0.460	0.460	0.460	0.460	0.460
$\bar{S}'_{wbr}$	0.203	0.387	0.567	0.599	0.634
$\bar{S}_{wbr}$	0.203	0.387	0.566	0.597	0.632
k_{ro}	0.940	0.940	0.940	0.940	0.940
$\bar{k}_{ro}$	0.585	0.0888	0.00650	0.00315	0.00136
k'_{ro}	0.605	0.179	0.0142	0.00252	0.00247
$\bar{k}_{rw}$	0.00611	0.0582	0.170	0.192	0.218
k'_{rw}	0.0086	0.0683	0.173	0.195	0.219
M'_1	0.354	0.743	2.54	4.49	9.94
M'_2	0.290	0.694	2.50	4.43	9.80
M'_3	0.251	0.633	2.50	4.43	9.87
M'_4	0.216	0.565	2.41	4.36	9.62
$N_{pbr} \times 10^6$	0.287	0.891	1.52	1.63	1.76
$V_p \times 10^6$	4.593	4.593	4.593	4.593	4.593
N_p/V_p	0.0625	0.194	0.330	0.356	0.384
S_{wi}	0.114	0.114	0.114	0.114	0.114
$(\bar{S}'_{wbr} - S_{wi})$	0.0892	0.273	0.452	0.483	0.518
E_{br}	70.1	71.2	73.1	73.6	74.1

Table 16 - Relative Permeability Curves 5

Displacement Results
"Darwin Sand, Wyoming"

	Results of Computer Runs				
	1	2	3	4	5
μ_o/μ_w	109	21.7	2.17	1.09	0.652
μ_o	50.0	10.0	1.00	0.500	0.300
μ_w	0.460	0.460	0.460	0.460	0.460
$\bar{S}'_{wbr}$	0.247	0.338	0.580	0.636	0.750
$\bar{S}_{wbr}$	0.247	0.339	0.580	0.636	0.750
k_{ro}	0.365	0.365	0.365	0.365	0.365
$\bar{k}_{ro}$	0.193	0.0592	0.00395	0.00210	0.000263
k'_{ro}	0.213	0.0919	0.00856	0.00393	0.00027
$\bar{k}_{rw}$	0.00441	0.0130	0.0517	0.0670	0.0741
k'_{rw}	0.00649	0.0163	0.0539	0.0687	0.114
M'_1	0.762	1.30	3.25	5.01	7.56
M'_2	0.543	1.07	3.14	4.87	7.52
M'_3	0.517	1.03	3.11	4.89	4.91
M'_4	0.397	0.508	2.90	4.64	4.89
$N_{pbr} \times 10^6$	0.215	0.546	1.45	1.68	2.12
$V_p \times 10^6$	5.058	5.058	5.058	5.058	5.058
N_p/V_p	0.0424	0.108	0.287	0.332	0.419
S_{wi}	0.187	0.187	0.187	0.187	0.187
$(\bar{S}'_{wbr} - S_{wi})$	0.0600	0.152	0.393	0.449	0.563
E_{br}	70.7	71.1	72.9	73.9	74.5

Table 17 - Relative Permeability Curves 6

Displacement Results
"Muddy Sand, Wyoming"

	Results of Computer Runs				
	1	2	3	4	5
μ_o/μ_w	109	21.7	10.9	1.09	0.652
μ_o	50.0	10.0	5.0	0.500	0.300
μ_w	0.460	0.460	0.460	0.460	0.460
$\bar{S}'_{wbr}$	0.397	0.433	0.461	0.592	0.650
$\bar{S}_{wbr}$	0.400	0.430	0.461	0.589	0.652
k_{ro}	0.425	0.425	0.425	0.425	0.425
$\bar{k}_{ro}$	0.0624	0.0385	0.0254	0.00321	0.000480
k'_{ro}	0.0671	0.04556	0.0334	0.0067	0.00297
$\bar{k}_{rw}$	0.0165	0.0222	0.0296	0.112	0.123
k'_{rw}	0.0173	0.0250	0.0335	0.123	*
M'_1	0.237	0.882	1.30	3.49	5.28
M'_2	0.229	0.817	1.21	3.40	5.25
M'_3	0.227	0.781	1.17	3.19	*
M'_4	0.219	0.721	1.07	3.04	*
$N_{pbr} \times 10^6$	0.702	0.855	0.975	1.55	1.78
$V_p \times 10^6$	5.617	5.617	5.617	5.617	5.617
N_p/V_p	0.125	0.152	0.174	0.275	0.317
S_{wi}	0.218	0.218	0.218	0.218	0.218
$(\bar{S}'_{wbr} - S_{wi})$	0.182	0.212	0.243	0.371	0.434
E_{br}	68.7	71.8	71.4	74.3	73.0

*No Data

Table 18 - Relative Permeability Curves 7
Displacement Results
"Dakota Sand, Wyoming"

	Results of Computer Runs				
	1	2	3	4	5
μ_o/μ_w	435	109	21.7	1.52	0.652
μ_o	200	50.0	10.0	0.700	0.300
μ_w	0.460	0.460	0.460	0.460	0.460
$\bar{S}'_{wbr}$	0.399	0.408	0.442	0.564	0.597
$\bar{S}_{wbr}$	0.400	0.411	0.439	0.566	0.599
k_{ro}	0.714	0.714	0.714	0.714	0.714
$\bar{k}_{ro}$	0.051	0.044	0.0252	0.00211	0.00103
k'_{ro}	0.0513	0.0463	0.0355	0.00497	0.00205
$\bar{k}_{rw}$	0.0109	0.0186	0.0256	0.102	0.129
k'_{rw}	0.0171	0.0202	0.0322	0.105	0.133
M'_1	0.151	0.353	1.28	4.59	8.46
M'_2	0.149	0.346	1.23	4.53	8.35
M'_3	0.0962	0.325	1.02	4.45	8.21
M'_4	0.0955	0.318	0.969	4.31	8.02
$N_{pbr} \times 10^6$	1.07	1.11	1.27	1.79	1.94
$V_p \times 10^6$	5.524	5.524	5.524	5.524	5.524
N_p/V_p	0.194	0.201	0.230	0.324	0.351
S_{wi}	0.121	0.121	0.121	0.121	0.121
$(\bar{S}'_{wbr} - S_{wi})$	0.279	0.290	0.318	0.445	0.478
E_{br}	69.6	69.3	72.4	72.9	73.5

Table 19 - Relative Permeability Curves 8
Displacement Results
"J-Sand, Nebraska"

	Results of Computer Runs				
	1	2	3	4	5
μ_o/μ_w	435	54.3	10.9	1.74	1.09
μ_o	200	25.0	5.0	0.80	0.50
μ_w	0.460	0.460	0.460	0.460	0.460
$\overline{S}'_{wbr}$	0.409	0.466	0.508	0.540	0.543
$\overline{S}_{wbr}$	0.409	0.466	0.508	0.539	0.543
k_{ro}	0.980	0.980	0.980	0.980	0.980
$\overline{k}_{ro}$	0.174	0.0444	0.00805	0.00124	0.000853
k'_{ro}	0.192	0.0812	0.0259	0.00257	0.00172
$\overline{k}_{rw}$	0.00396	0.0212	0.0605	0.116	0.124
k'_{rw}	0.00493	0.0253	0.0651	0.118	0.126
M'_1	0.569	0.850	1.49	4.87	7.26
M'_2	0.517	0.818	1.47	4.84	7.21
M'_3	0.457	0.714	1.38	4.76	7.15
M'_4	0.420	0.674	1.34	4.70	7.06
$N_{pbr} \times 10^6$	0.427	0.649	0.822	0.964	0.982
$V_p \times 10^6$	5.40	5.40	5.40	5.40	5.40
N_p/V_p	0.0790	0.120	0.152	0.179	0.182
S_{wi}	0.297	0.297	0.297	0.297	0.297
$(\overline{S}'_{wbr} - S_{wi})$	0.112	0.169	0.211	0.242	0.246
E_{br}	70.7	71.2	72.2	73.7	73.8

Table 20 - Relative Permeability Curves 9
Displacement Results
"D-Sand, Nebraska"

	Results of Computer Runs				
	1	2	3	4	5
μ_o/μ_w	435	21.7	10.9	1.63	0.870
μ_o	200	10.0	5.00	0.750	0.400
μ_w	0.460	0.460	0.460	0.460	0.460
$\bar{S}'_{wbr}$	0.190	0.422	0.495	0.677	0.709
$\bar{S}_{wbr}$	0.189	0.422	0.493	0.678	0.710
k_{ro}	0.927	0.927	0.927	0.927	0.927
$\bar{k}_{ro}$	0.617	0.108	0.0269	0.00217	0.00115
k'_{ro}	0.633	0.228	0.146	0.0142	0.00556
$\bar{k}_{rw}$	0.00571	0.0758	0.121	0.298	0.333
k'_{rw}	0.0083	0.092	0.140	0.307	0.335
M'_1	0.373	0.563	0.705	1.91	3.20
M'_2	0.299	0.528	0.691	1.90	3.19
M'_3	0.258	0.464	0.607	1.85	3.18
M'_4	0.219	0.416	0.557	1.80	3.12
$N_{pbr} \times 10^6$	0.560	1.72	2.09	3.08	3.27
$V_p \times 10^6$	7.044	7.044	7.044	7.044	7.044
N_p/V_p	0.0795	0.244	0.297	0.437	0.464
S_{wi}	0.077	0.077	0.077	0.077	0.077
$(\bar{S}'_{wbr} - S_{wi})$	0.112	0.345	0.416	0.601	0.633
E_{br}	71.0	70.8	71.4	72.7	73.3

Table 21 - Relative Permeability Curves 10
Displacement Results

"Curve 10"

	Results of Computer Runs				
	1	2	3	4	5
μ_o/μ_w	217	21.7	10.9	1.52	0.650
μ_o	100	10.0	5.00	0.700	0.300
μ_w	0.460	0.460	0.460	0.460	0.460
$\bar{S}'_{wbr}$	0.235	0.348	0.381	0.498	0.542
$\bar{S}_{wbr}$	0.237	0.347	0.380	0.496	0.540
k_{ro}	0.946	0.946	0.946	0.946	0.946
$\bar{k}_{ro}$	0.274	0.0884	0.0517	0.00252	0.00104
k'_{ro}	0.296	0.1132	0.0827	0.0180	0.00732
$\bar{k}_{rw}$	0.00867	0.0601	0.0888	0.231	0.299
k'_{rw}	0.0113	0.0720	0.101	0.242	0.303
M'_1	0.502	0.724	0.980	2.69	4.86
M'_2	0.438	0.678	0.931	2.68	4.83
M'_3	0.386	0.603	0.860	2.57	4.79
M'_4	0.345	0.562	0.800	2.45	4.61
$N_{pbr} \times 10^6$	1.07	1.90	2.17	3.10	3.48
$V_p \times 10^6$	10.43	10.43	10.43	10.43	10.43
N_p/V_p	0.102	0.183	0.208	0.298	0.333
S_{wi}	0.090	0.090	0.090	0.090	0.090
$(\bar{S}'_{wbr} - S_{wi})$	0.147	0.257	0.290	0.406	0.450
E_{br}	69.7	71.1	71.5	73.3	74.1

Legend for Figures 5, 6, and 8 through 12.

Relative Permeability Curves

1 (△)

2 (○)

3 (◇)

4 (▯)

5 (▽)

6 (▲)

7 (●)

8 (◆)

9 (▮)

10 (▼)

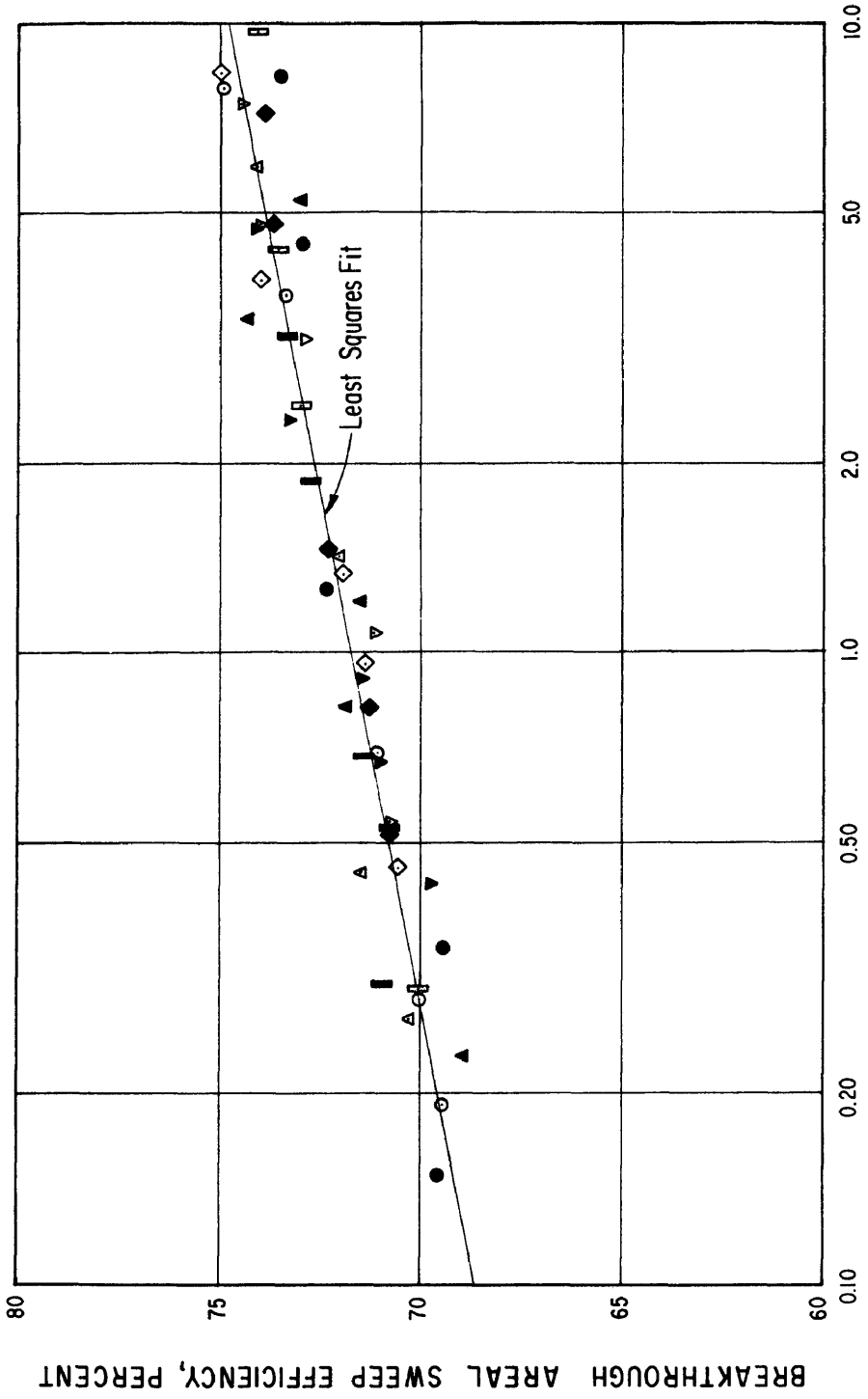

FIGURE 5. CORRELATION BETWEEN BREAKTHROUGH AREAL SWEEP EFFICIENCY AND MOBILITY RATIO M_2'.

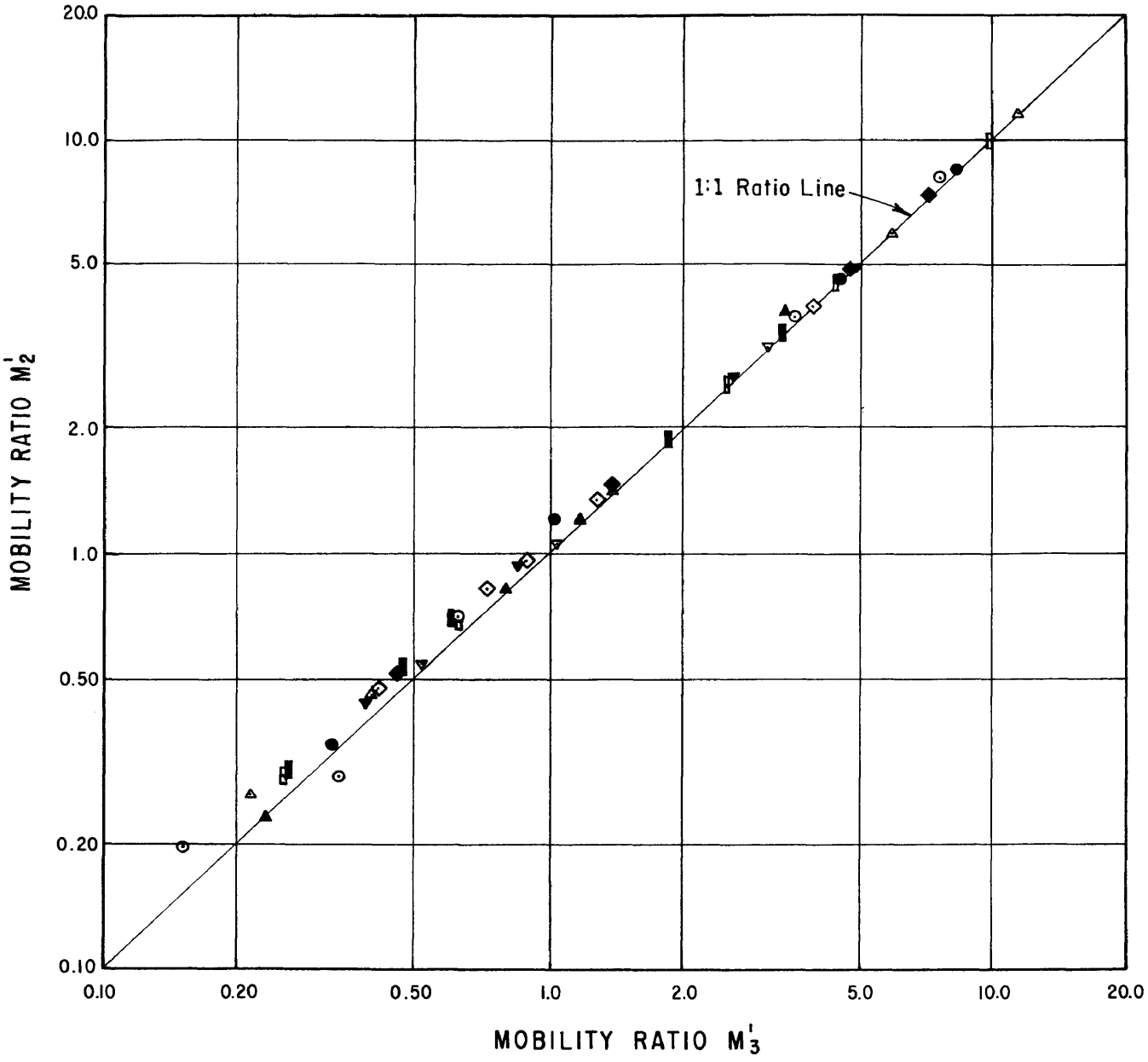

FIGURE 6. COMPARISON OF MOBILITY RATIO M_2' WITH MOBILITY RATIO M_3'.

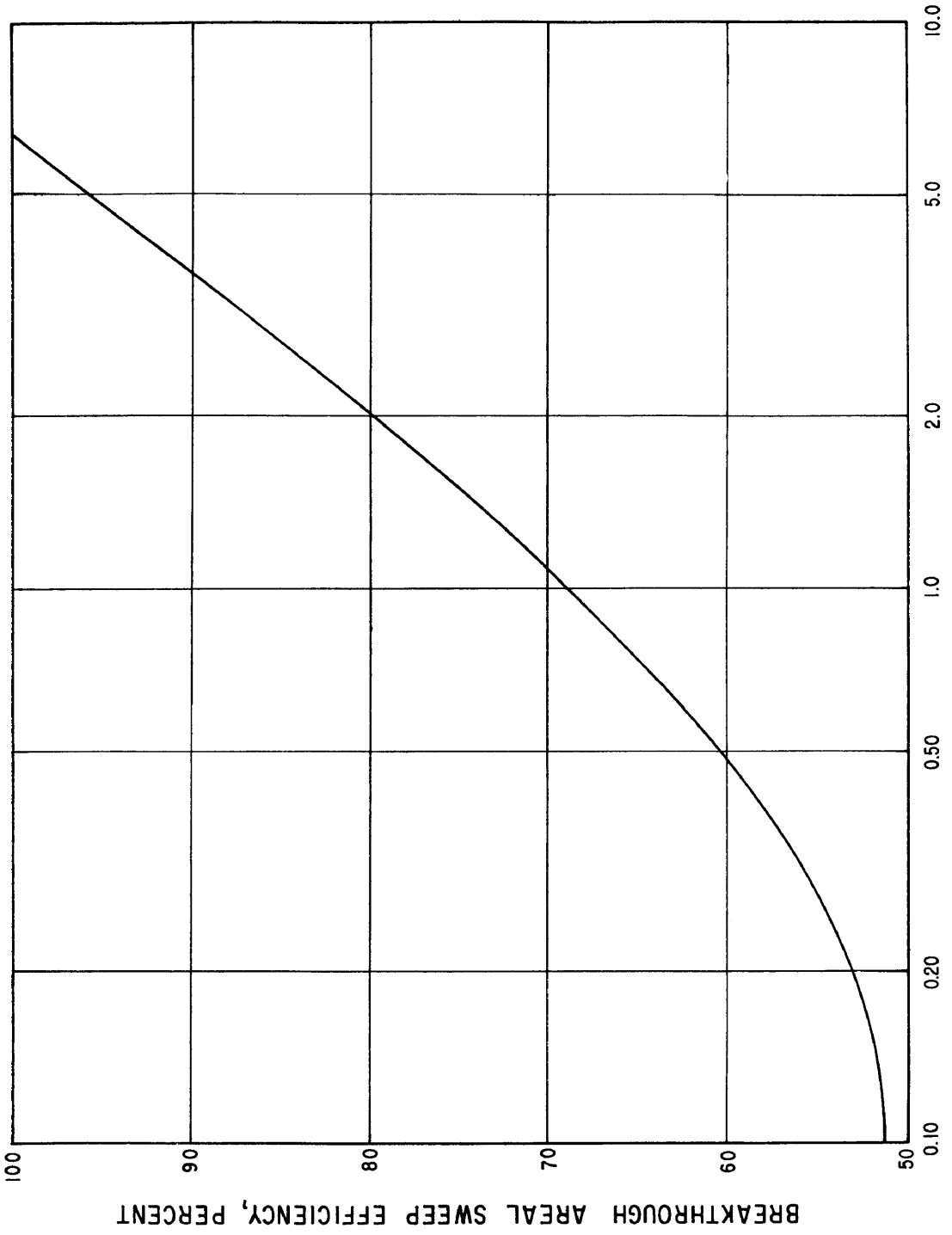

FIGURE 7. CORRELATION OF BREAKTHROUGH AREAL SWEEP EFFICIENCY WITH MOBILITY RATIO M_3'. From Craig, Geffen and Morse (1955, p. 9).

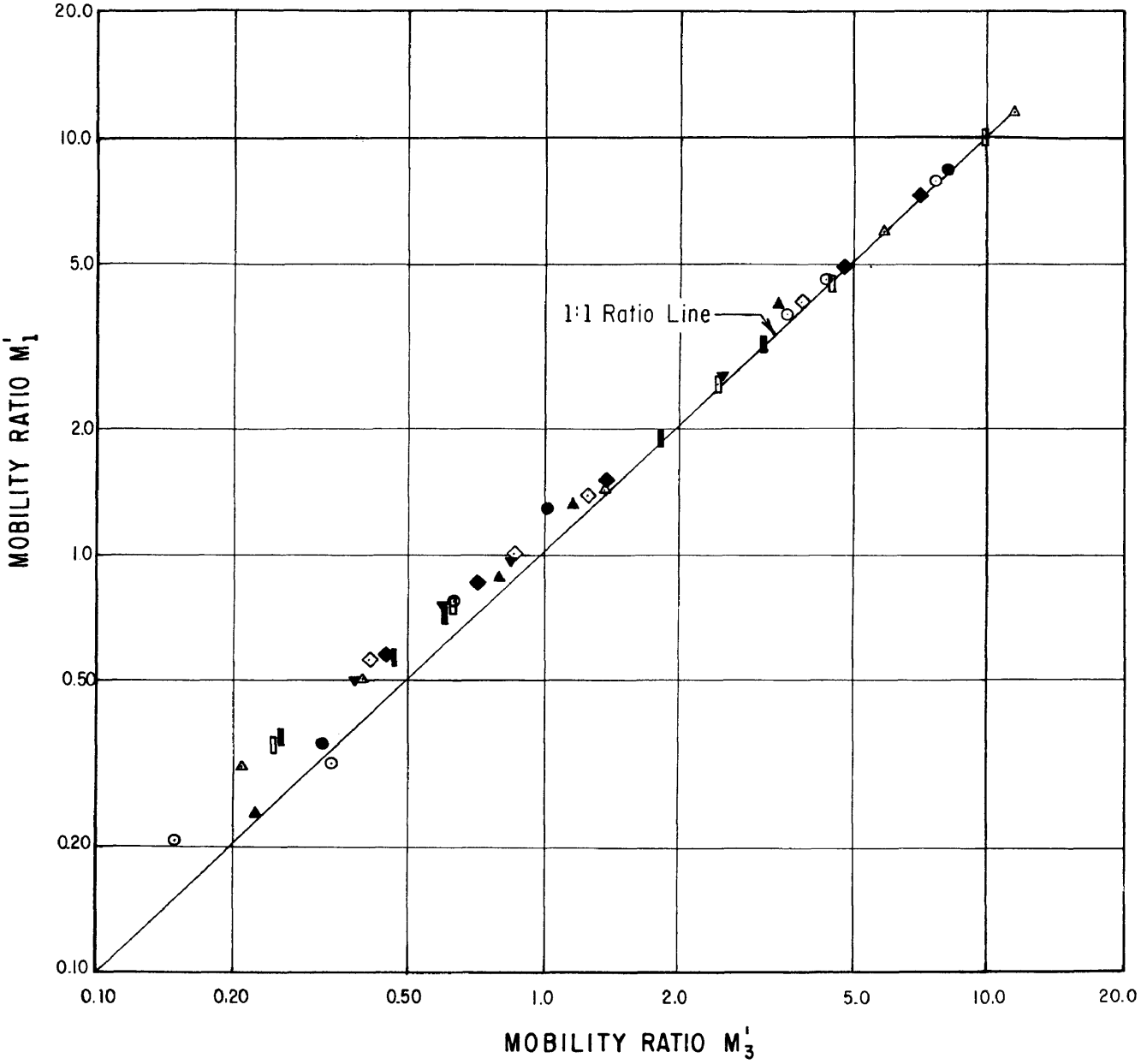

FIGURE 8. COMPARISON OF MOBILITY RATIO M_1' WITH MOBILITY RATIO M_3'.

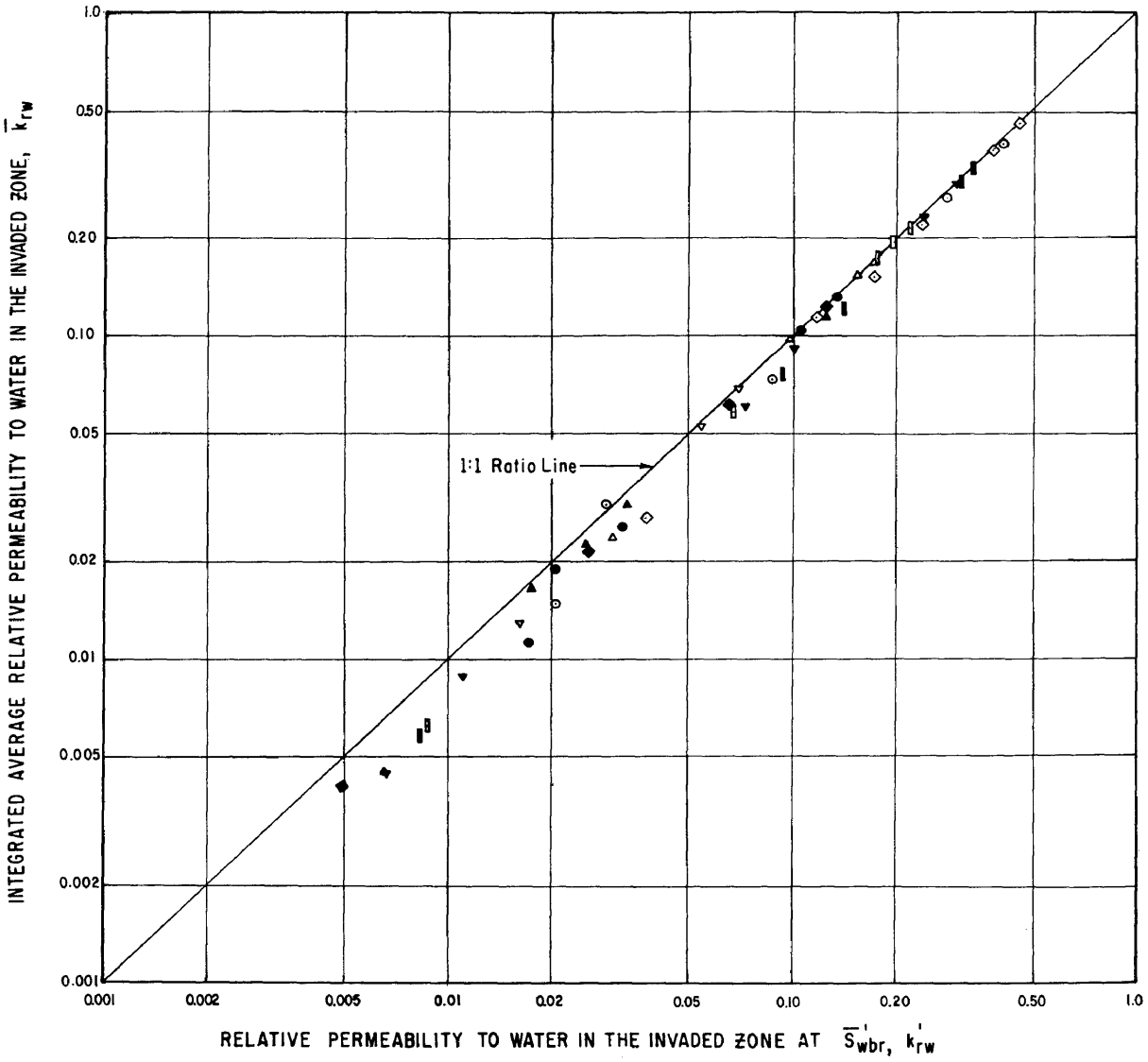

FIGURE 9. COMPARISON OF THE AVERAGE RELATIVE PERMEABILITY TO WATER IN THE INVADED ZONE CALCULATED BY TWO DIFFERENT METHODS.

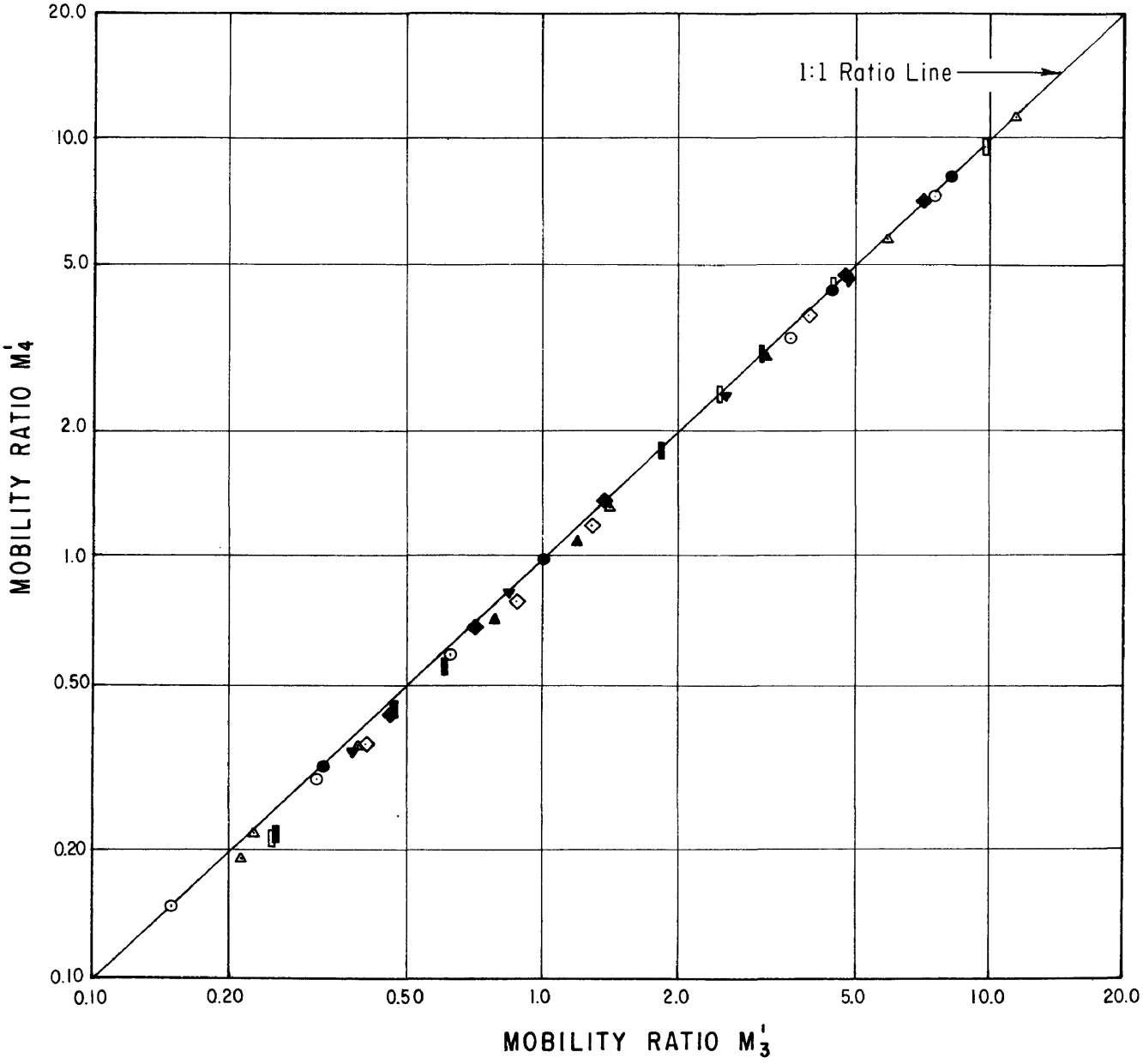

FIGURE 10. COMPARISON OF MOBILITY RATIO M_4' WITH MOBILITY RATIO M_3'.

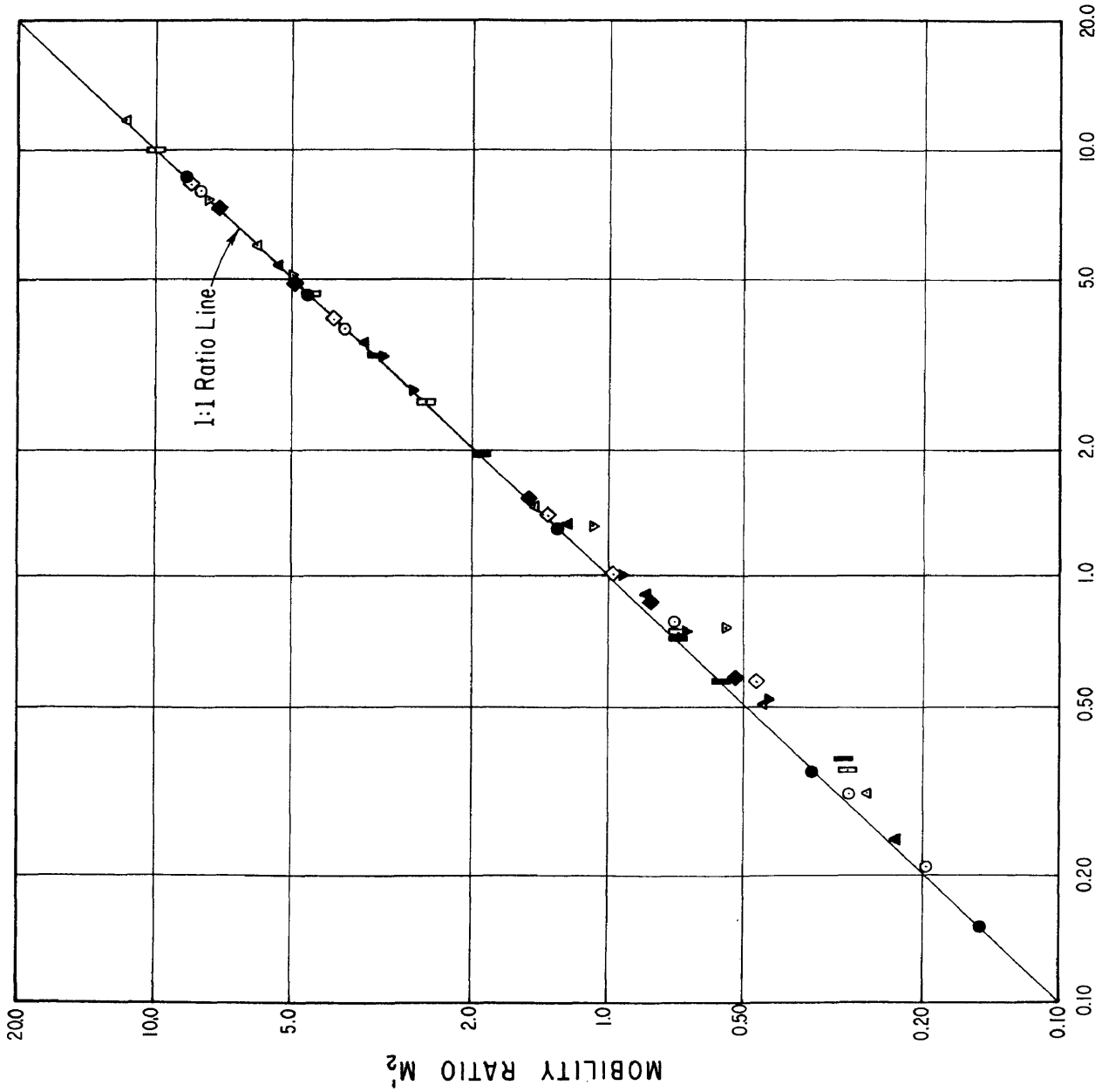

FIGURE 11. COMPARISON OF MOBILITY RATIO M_2' WITH MOBILITY RATIO M_1'.

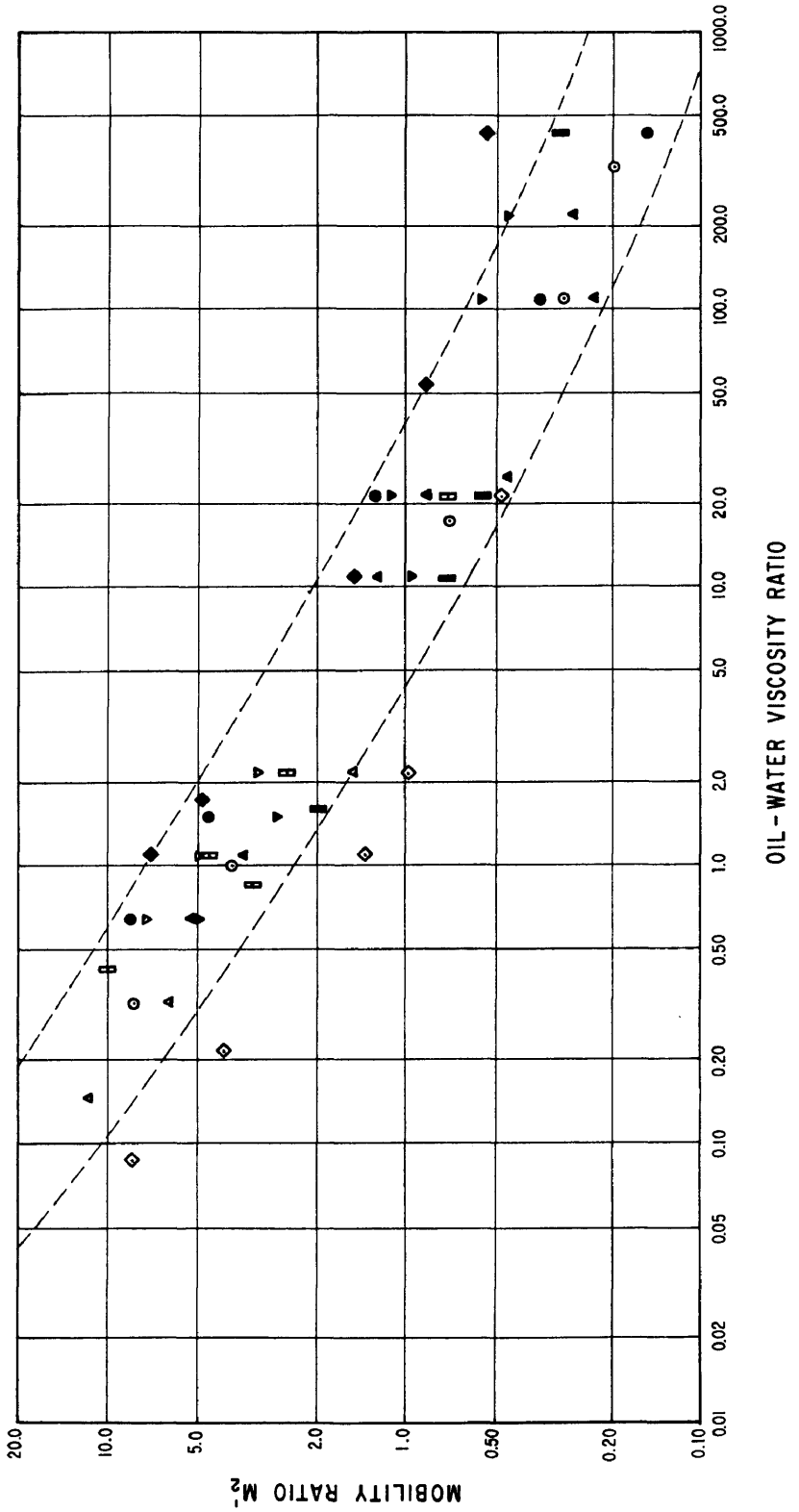

FIGURE 12. CORRELATION OF MOBILITY RATIO M_2' WITH OIL-WATER VISCOSITY RATIO.

BIBLIOGRAPHY

Aronofsky, J.S., 1952, Mobility Ratio - its influence on flood patterns during water encroachment: Petroleum Transactions, AIME, v. 195, p. 15-24.

Aronofsky, J. S. and Ramey, H. J. Jr., 1956, Mobility Ratio - its influence on injection or production histories in five-spot water flood: Petroleum Transacations, AIME, v. 207, p. 205-210.

Caudle, B. H., Erickson, R. A. and Slobod, R. L., 1955, The encroachment of injected fluids beyond the normal well pattern: Petroleum Transactions, AIME, v. 204, p. 79-85.

Cheek, Rex E. and Menzie, Donald E., 1955, Fluid mapper model studies of mobility ratio: Petroleum Transactions, AIME, v. 204, p. 278-281.

Cotman, Nathan T., Still, Gerald R. and Crawford, Paul B., 1962, Laboratory comparison of oil recovery in five-spot and nine-spot waterflood patterns: Producers Monthly, vol. 26, December, p. 10-13.

Craig, F. F. Jr., Geffen, T. M. and Morse, R. A., 1955, Oil recovery performance of pattern gas or water injection operations from model tests: Petroleum Transactions, AIME, v. 204, p. 7-15.

Douglas, Jim, Jr., Peaceman, D. W. and Rachford, H. H., 1959, A method for calculating multi-dimensional immiscible displacement: Petroleum Transactions, AIME, v. 216, p. 297-308.

Dyes, A. B. and Braun, Philip H., 1954, Sweepout Patterns in depleted and stratified reservoirs: Producers Monthly, v. 19, December, p. 24-30.

Dyes, A. B., Caudle, B. H. and Erickson, R. A., 1954, Oil production after breakthrough as influenced by mobility ratio: Petroleum Transactions, AIME, v. 201, p. 81-85.

Higgins, R. V. and Leighton, A. J., 1961, Performance of five-spot water floods in stratified reservoirs using streamlines: Paper SPE-57 presented at the Rocky Mountain Regional Meeting of SPE in Farmington, N.M., (May 25-26, 1961).

_____ 1962, A computer method to calculate two-phase flow in any irregularly bounded porous medium: Petroleum Transactions, AIME, v. 225, p. 679-683.

_____ 1962, Computer prediction of water drive of oil and gas mixtures through irregularly bounded porous media - three-phase flow: Petroleum Transactions, AIME, v. 225, p. 1048-1054.

Higgins, R. V. and Leighton, A. J., 1963, Principles and computer techniques for calculating performance of a five-spot waterflood - two-phase flow: U. S. Bureau of Mines, RI-6305.

Nobles, M. A. and Janzen, Harold B., 1958, Application of a resistance network for studying mobility ratio effects: Petroleum Transactions, AIME, v. 213, p. 356-358.

Rapoport, L. A., Carpenter, C. W., Jr. and Leas, W. J., 1958, Laboratory studies of five-spot waterflood performance: Petroleum Transactions, AIME, v. 213, p. 113-120.

Slobod, R. L. and Caudle, B. H., 1952, X-Ray shadowgraph studies of areal sweepout efficiencies: Petroleum Transactions, AIME, v. 195, p. 265-270.